Environmental Research Center Papers

NUMBER 13

1990

Environmental Research Center
The University of Tsukuba

A LOCAL CLIMATOLOGICAL STUDY ON THE MECHANICS OF NOCTURNAL COOLING IN PLAINS AND BASINS*

By Hitoshi Toritani**

(received 31 January, 1990)

ABSTRACT

At clear and calm nights, the air near the ground surface is cooled mainly due to radiative processes, thus an inversion layer is formed near the surface. In a basin, a strong surface inversion layer is formed and extraordinary low air temperature occurs at the bottom of it.

Analysis of the difference of the structures and mechanics of the atmospheric cooling on a plain versus in a basin was done with field observations in the Sugadaira Basin, Nagano Prefecture, and with data obtained at the Environmental Research Center, University of Tsukuba, and Meteorological Research Institute and Aerological Observatory located in Tsukuba Science City, Ibaraki Prefecture.

Compared with the difference of time variations of the air temperature in the surface inversion layer formed at a night, between on a plain and in a basin, the observed cooling in the basin was estimated to be about 1.4 times higher than on the plain. In detail, radiative cooling in the basin was about 1.3 times higher, and turbulent and advective cooling in it were about twice higher than on the plain. It is because the basin was located in the place with high altitude that radiative cooling was higher in the basin. On the other hand, it is because the basin had the slopes surrounding it, where cold air was formed, and because this cold air was transferred along the slope to the air layer above the bottom of the basin, that turbulent and advective coolings were about twice higher in the basin.

---

* A dissertation submitted in partial fulfillment of the requirements for the degree of Doctor of Science in Doctoral Program in the University of Tsukuba.

** Present address, Department of Geoscience, National Defense Academy, 239 Kanagawa, Japan

CONTENTS

ABSTRACT 1

LIST OF FIGURES 3

LIST OF TABLES 5

CHAPTER I INTRODUCTION 6
1.1 Purpose of this study 6
1.2 Review of recent studies 6

CHAPTER II METHODS OF OBSERVATIONS AND ACQUISITIONS OF DATA 10
2.1 Observations and acquisitions of data at Tsukuba 10
2.2 Observations and acquisitions of data in Sugadaira 11

CHAPTER III STRUCTURES AND MECHANICS OF NOCTURNAL COOLING ON A PLAIN . 13
3.1 Characteristics of nocturnal cooling on a plain 13
3.2 The structure of the surface inversion layer formed on a plain 17
3.3 Methods of analysis of variation of air temperature in the surface inversion layer formed in the nighttime 20
3.4 The atmospheric cooling in the surface inversion layer formed on a plain 23

CHAPTER IV STRUCTURES AND MECHANICS OF NOCTURNAL COOLING IN A BASIN . 25
4.1 The structure of the surface inversion layer formed at the bottom of a basin 25
4.2 The structure of the surface inversion layer formed on a slope 27
4.3 The atmospheric cooling in a cold air lake and cold air drainage formed in a basin . 31
4.4 The atmospheric circulation and cooling when cold air lake and cold air drainage are formed in a basin 36

CHAPTER V GEOGRAPHICAL CHARACTERISTICS OF NOCTURNAL COOLING 42
5.1 The characteristics of nocturnal cooling in the Kanto District 42
5.2 The relationships between topographical features and nocturnal cooling in basins in the Tohoku and Chubu Districts 45

CHAPTER VI DISCUSSION 54

CHAPTER VII CONCLUSIONS 57

ACKNOWLEDGEMENTS 58

REFERENCES 59

LIST OF FIGURES

Figure		Page
2.1	Maps of Tsukuba	10
2.2	A map of Sugadaira	12
2.3	Measurement sites (P1~P8) at the experimental slope in Sugadaira basin	12
3.1	The definition of cooling rate (observed at E.R.C. for May 21–22, 1986)	13
3.2	The seasonal variations of cooling rate, net radiation and wind speed at 1.6 m high at the Environmental Research Center, University of Tsukuba for 1981–1987	14
3.3	The relationships of net radiation and cooling rate. Wind speed: (a) 0.0–0.5 (m/s), (b) 0.5–1.0 (m/s), (c) 1.0–2.0 (m/s) and (d) more than 2.0 (m/s)	15
3.4	The relationships between net radiation, and (a) downward and (b) upward long wave radiations at E.R.C. for May, 1982	16
3.5	Temporal variations in amount of cloud cover, downward long-wave radiation and air temperatures in the upper layer for May, 1982	17
3.6	Time variations of surface and air temperatures at 1.6 m high and wind direction and speed at 10 m high. (a) May 7–8 and (b) May 9–10, 1982	18
3.7	Time variations of surface and air temperatures at 7 heights. (a) May 7–8 and (b) May 9–10, 1982	19
3.8	Time variations of wind speed at 7 heights. (a) May 7–8 and (b) May 9–10, 1982	19
3.9	Vertical profiles of the air temperature and time and height section of wind direction and speed on May 7–8, 1982. (a) Vartical profiles and (b) time and height section	19
3.10	Same as Fig. 3.9, but May 9–10, 1982	20
3.11	The comparison between measured and calculated values of the integrated values of net radiation between 1900 and 0500 on 7 nights mentioned in Table 3.3	22
3.12	Vertical distributions of the net radiation obtained from the methods mentioned in Chapter 3–3. (a) May 7–8 and (b) May 9–10, 1982	22
3.13	Time variations of air temperature in the lst, 2nd and 3rd sub-layers on a plain on May 7–8, 1982	23
3.14	Same as Fig. 3.13, but on May 9–10, 1982	23
3.15	Time variations of air temperature in the lst, 2nd and 3rd sub-layers on a plain on 7 nights	24
4.1	Time variations of wind and air temperature at the bottom of the basin. (a) May 7–8 and (b) May 9–10, 1982	25
4.2	Time variations of air temperature above the bottom of the basin. (a) May 7–8 and (b) May 9–10, 1982	25
4.3	Vertical profiles of air temperature and time and height sections of wind direction and speed above the bottom of the basin on May 7–8, 1982. (a) Vertical profiles and (b) time and height section	26
4.4	Same as Fig. 4.3, but for May 9–10, 1982	26
4.5	Time variations of air temperature at the bottom of the basin and on the slope of Mt. Omatsu. (a) May 7–8 and (b) May 9–10, 1982	27
4.6	Isopleth of air temperature at the bottom of the basin and on the slope of Mt. Omatsu from 1800 May 7 to 0700 May 8, 1982	28

4.7 Same as Fig. 4.6, but from 1800 May 9 to 0700 May 10, 1982 28
4.8 Same as Fig. 4.6, but from 1800 Oct. 3 to 0700 Oct. 4, 1982 29
4.9 Same as Fig. 4.6, but from 1800 June 11 to 0700 June 12, 1984 29
4.10 Time variations of air temperature and wind speed on the slope of Mt Omatsu. (a) May 7–8 and (b) May 9–10, 1982 30
4.11 Time variations of air temperature on and above the slope. (a) May 7–8 and (b) May 9–10, 1982 30
4.12 Vertical profiles of air temperature on and above the slope. (a) May 7–8 and (b) May 9–10, 1982 31
4.13 Vertical distributions of net radiation in the air layer between the ground surface and at a height of 200 m at the nights on May 7–8 and 9–10, 1982 32
4.14 Time variations of air temperature in the three sub-layers at the night on May 7–8, 1982 33
4.15 Same as Fig. 4.14, but at the night on May 9–10, 1982 33
4.16 Time variations of air temperature in the air layer between the ground surface and 100 m level above the slope at the night on May 7–8, 1982 34
4.17 Same as Fig. 4.16, but at the night on May 9–10, 1982 35
4.18 The nocturnal mean of the variations of air temperature in the air layer from the surface to 200 m high at the bottom of the basin and from the surface to 100 m high on the slope on May 7–8 and 9–10, 1982 36
4.19 Time variations of wind and potential temperature above the bottom of the basin and on and above the slope at the night on May 7–8, 1982. The arrows denote the wind direction and speed obtained above the bottom of the basin 37
4.20 Same as Fig. 4.19, but at the night on May 9–10, 1982 37
4.21 Vertical cross sections of potential temperature at the first stage. (a) May 7–8 and (b) May 9–10, 1982 38
4.22 Same as Fig. 4.21, but at the second stage 39
4.23 Same as Fig. 4.21, but at the third stage 40
4.24 The variations of air temperature above the bottom of the basin at each stage on May 7–8 and 9–10, 1982 41
5.1 Observation points of the AMeDAS in the Kanto Plain 42
5.2 The spatial distribution of the monthly averaged cooling rate (℃/h) for May, 1986 . . . 43
5.3 The spatial distribution of wind direction of the highest frequency and the monthly averaged wind speed (m/s) for May,1986 43
5.4 The relationships between clear-night index and net radiation through the night at the Aerological Observatory for May, 1986 44
5.5 The spatial distribution of clear-night index (h) in Kanto District for May, 1986 44
5.6 The relationships between clear-night index and cooling rate in the Kanto District for May, 1986 45
5.7 A simple model indicating the shape of the basin 46
5.8 The locations of the basins analysed in Tohoku and Chubu Districts 46
5.9 The relationships between cooling rate and height above sea level at the bottom of the basin 51
5.10 The relationship between S_s/S_b and cooling rate at the bottom of the basins 52
5.11 The relationship between $tan\ \alpha$ and cooling rate at the bottom of the basins 53

LIST OF TABLES

Table		Page
1.1	The thickness of the stable layer formed in basins and valleys	7
2.1	The observed parameters and instruments used at each observation site	11
2.2	The data periods and instrumentation in Sugadaira	12
3.1	The correlation between cooling rate and other meteorological components	14
3.2	The relationships of net radiation and various wind speeds at 1.6 m	16
3.3	The days selected to consider variations of air temperature at night	21
5.1	The parameters of the shape of the basins ((Tohoku District) and (Chubu and Kanto District))	47
5.2	The slope angle α and the exposure to the sky β of the surrounding slope ((Tohoku District), and (Chubu and Kanto District))	49
5.3	The correlations between geographical shapes and cooling rate in basins	51
6.1	Nocturnal mean values of cooling rate and wind speed in the surface inversion layers on a plain (Tsukuba) and in a basin (Sugadaira) (May 7–10, 1982)	54
6.2	Monthly mean values of cooling rate and nocturnal wind speed near the earth's surface on plains and in basins in the Kanto district (May, 1986)	54
6.3	Nocturnal mean values of heat balance components indicated by the variation of air temperature in the surface inversion layers on the plain (Tsukuba) and in the basin (Sugadaira) (May 7–10, 1982)	55
6.4	Nocturnal mean values of heat balance components indicated by the variation of air temperature in the surface inversion layers on and above the slope at Sugadaira (May 7–10, 1982)	56

CHAPTER I

INTRODUCTION

1.1 Purpose of this study

At nights, the air near the ground is cooled due to radiative heat loss from the ground surface and from the air itself. The intensity of this atmospheric cooling depends on meteorological conditions, topography and ground surface conditions.

On clear and calm nights, the cooling of the air near the surface is strong and the minimum air temperature which occurs just before or after sunrise is lower than that at other times of the morning (Nishiyama, 1985). Moreover air temperature is the lowest near the surface and increases with height. This condition is called surface inversion or ground inversion.

In a basin, strong surface inversion layer is formed above the bottom of the basin. On the slope surrounding the basin, air parcel moves into a topographically lower place due to gravitational forces. This strong surface inversion layer and air flow are the characteristic phenomena formed in a basin area on clear and calm nights. The former is called cold air lake and the latter cold air drainage. When these phenomena occur in a basin area, the air layer on and above the bottom of the basin is cooled strongly and so extraordinary low air temperratures occur near the surface at the bottom of the basin.

The purposes of the present study are first to clarify the characteristics of atmospheric cooling near the surface at night. Secondly, the difference of the structures and mechanics of the atmospheric cooling between a plain versus a basin are clarified. Simultaneously, the relationships between the strong atmospheric cooling, and the cold air lake and cold air drainage are clarifind. Finally, the relationships between the intensity of atmospheric cooling at night and topographical conditions are explained.

1.2 Review of recent studies

On clear and calm nights, a surface inversion layer is formed near the surface due primarily to strong radiative cooling. One of the characteristics of the inversion layer is its thickness. Tosha (1953) and Ota (1960) reported that the thickness of the surface inversion layer on a plain was 150 to 250 m high. At Tateno, located in the eastern part of the Kanto Plain, the thickness of the stable layer was 100 to 200 m above ground level (AGL) (Ishibashi and Numata, 1965; Suzuki, 1977; Suzuki *et al.*, 1978). Mano (1953) stated that the thickness of the surface inversion layers, influenced by surrounding mountains, were generally lower than those formed over a plain. For instance, the thickness of the surface inversion formed in a valley surrounded by mountains was 50–70 m high, but on the coast, it reached 100–200 m high.

Results of the recent studies on the thickness of the inversion layer formed in basins and valleys in Japan are shown in Table 1.1. This table indicates the thickness of the surface inversion layer was mostly between 100 to 300 m high and the ratio of the thickness of surface inversion layer to the relative height of surrounding peaks was 0.4 to 1.0. These values coincide with the previous ones deduced from the results in the world (Yoshino, 1975).

There are several numerical and theoretical methods of defining the thickness of inversion layer (Hanna, 1969; Wyngaard, 1975; Yu, 1978; Zeman, 1979; Nieuwstadt and Tennekes, 1981). These methods indicate that the surface inversion layer becomes thicker with increasing friction velocity, wind speed at the top of the inversion layer and atmospheric stability. Kondo and Kuwagata (1984) also summarized the relationships between the thickness of inversion layer formed in basins and valleys, and the relative height of

Table 1.1 The thickness of the stable layer formed in basins and valleys.

(1)	(2)	(3)	(4)	(5)	(6)	(7)	(8)	(9)
Aizu, Fukushima	200	1,300	1,100	400	0.35	Nov. 29–30, 1978	*1	Nomoto, 1982
Kyoto	10	460	450	450	1.00	Oct. 19–20, 1981	*3	Tanaka, 1984
Sugadaira, Nagano	1,250	1,450	200	90–120	0.45–0.60	May 8, 1981	*2	Kudo et al., 1982
				80–120	0.40–0.60	Aug. 25–28, 1980	*2	Nakamura et al., 1985
Moshiri, Hokkaido	290	500	210	120	0.57	Feb. 9–10, 1980	*2	Magono et al., 1982
				>100	>0.48		*2	Maki et al., 1984
				140	0.67		*2	〃
				150–160	0.71–0.76		*4	Taniguchi et al., 1983
Akaigawa, Hokkaido	150	400	350	360	1.03	Oct. 22–23, 1982	*2	Harimaya et al., 1985
				340	0.93	Oct. 22–23, 1982	*4	〃
Saku, Nagano	540	1,890	1,350	800	0.59	Jul. 28, 1983	*3,*1	Tanaka and Edagawa, 1985
						Aug. 1, 1984	*3,*1	

(1) Location
(2) Altitude of the bottom of the basin, the valley floor and the mountain foot (m above sea level).
(3) Altitude of the surrounding ridges or peaks (m above sea level).
(4) Relative elevation of the basin and valley (m).
(5) Thickness of the stable layer formed in the basin and valley (m).
(6) Ratio of the thickness of the stable layer and the elevation of the basin and valley.
(7) Observation period.
(8) Instrumentation.
*1 pilot balloon
*2 tethered balloon
*3 tethered sonde
*4 sonic rader
(9) Source

the surrounding peaks from the results of observations in Japan. They found as follows; (1) The thickness of the surface inversion layer and the relative height of the surrounding peaks was almost equal, that is, the thickness of the surface inversion layer reached the relative height of the surrounding peaks. (2) There was a proportional relation between the thickness of the surface inversion layer and the relative height of the surrounding peaks. Schroeder and Buck (1970) pointed out that surface inversion layers were more common and more intense in mountain valleys and basins than over flat areas, thus extraordinary cooling which occurred in a basin was considered to be related not to thickness but to the strength of surface inversion layer.

The strong inversion layer (cold air lake) formed in a basin is considered to be part of the circulation formed in mountains, valleys and basins. (Mano, 1953; Mano, 1956; Vorontsov, 1958a, b, 1969; Kimura, 1961; Yoshino 1975; Kudo *et al.*, 1982). Geiger (1965) stated that the cold air lake was mainly formed by the cold air drainage from the surrounding slope to the basin. Conversely, Miura (1971) showed, based on observations in the Sugadaira Basin, Japan, that the formation of cold air lake was due to radiative cooling at the surface of the basin. Magono and Nakamura (1982) observed the Moshiri Basin, in northern Hokkaido in midwiter and stated that the cold air drainage flowed directly toward the bottom of the basin only for several hours after sunset. After this cooling stage, a cold air lake was formed mainly by the cooling of surface air due to the heat exchange with the extremely cooled surface of snow cover.

There are also some reports about the relationships of extraordinary drops of air temperature and cold air lake and cold air drainage. Kondo (1982), Mori *et al.*, (1983), Harimaya *et al.* (1985) clarified that the advection and accumulation of cold air over the central part of a basin were important factors of nocturnal cooling in the basin and the formation of a cold air lake. Maki *et al.* (1985a, b, 1986) stated that the cooling rate at the surface of the Akaigawa Basin, in western part of Hokkaido, was high, because the cold air drainage advected and accumulated over the bottom of the basin. This was because the advection and accumulation of the cold air drainage reduced the amount of downward longwave radiation and thus strengthened the radiative cooling at the surface of the basin.

As mentioned above, cold air drainage plays an important role in nocturnal cooling in a basin. Cold air drainage is an air stream which is formed by radiative cooling on a slope and flows down along the slope due to gravity (Baumgartner, 1963; Geiger, 1965; Yoshino, 1975, 1980). Thus, velocity of cold air drainage is related to the atmospheric cooling and gravity. There are several theoretical studies about this. Fleagle (1950) studied the effects on drainage velocity of slope angle, friction and the non-adiabatic cooling rate of the slope air. Petkovšek and Hočevar (1971) expressed the velocity of the cold air drainage by assuming that, in the steady state case, acceleration of the cooled slope air due to gravity was balanced by friction. Sahashi (1974) made it clear that the velocity of cold air parcel along the slope changed periodically with the distance from the top of the slope, on the assumption that the air parcel had compressibility and the friction force was proportional to the falling velocity of the parcel.

Bergen (1969) indicated that wind speed varied in a nearly linear manner down the slope in an observation on a small forested slope. Ohata and Higuchi (1979) reported that cold air drainage formed in a snow patch in the Central Japan on early summer days. They showed that the wind speed of cold air drainage was stronger at lower parts of the snow patch. Wind speed was in direct proportion to the square root of the distance from the upper end of the snow patch. Kondo (1984) clarified from the parcel model that the speed of cold air depended on the potential temperature difference between the surface and the cooled air layer, and on the distance at which the cold air drainage flows on the slope.

The wind speed cold air drainage is considered to be related to the amount of the supply of cold air to cold air lake and also to the cooling in the air layer above the bottom of the basin. Regarding variations of wind speed and air temperature with time, Nakamura (1976) reported that falling air temperature was

inversely proportional to wind speed with a correlation coefficient of −0.9. Yoshino *et al.* (1981) made it clear that the correlation between wind speed and air temperature was negative with coefficients ranging from −0.88 to −0.84 when cold air drainage occurred on the slope. Tanaka *et al.* (1982) showed that comparing the periodic variations of wind speeds with those of air temperatures, weak wind gusts were found to be accompanied by the decrease of air temperature near the ground surface. Maki *et al.* (1984) and Harimaya *et al.* (1985) showed that the cooling rate on a slope agreed well with the speed of cold air drainage, and that the period of the highest cooling rate was in accordance with that of the highest speed of it.

As mentioned above, wind speed and air temperature are periodical, because cold air drainage moves periodically. Aichele (1953) confirmed the periodicity of cold air drainage by means of observations of the fog in the Salemer Valley, north of Lake Constance. Buettner and Thyer (1966) found a periodicity of about 25 minutes with a range from 1.5 to 6.5 m/s in the Carbon River Valley. Tyson (1968) revealed, by a spectral analysis, that velocity changed from 1.0 to 4.0 m/s with a periodicity of 75 minutes in the Drakensberg Foothills near Pietermaritzburg, South Africa. Doran and Horst (1981) reported that variation of velocity and air temperature of cold air drainage had a periodicity of 1 to 1.5 h in the Geysers area of northern California. Kobayashi and Ishikawa (1982) clarified the wavy motion of cold air drainage, and the phenomena of wind turbulence and air temperature on the snow surface from the observations carried up in the mist and cold air layer in Hokkaido. Toritani (1985) reported that the fluctuation of wind speed and air temperature appeared as surges with periods ranging from 40 to 60 minutes when cold air drainage flowed down on a slope in the Sugadaira Basin.

As a conclusion of the present review, it is summarized that there have been many reports about the characteristics of cold air lake and cold air drainage, but there are only a few reports about the relationships between the atmospheric cooling, and cold air lake and cold air drainage in various basins. There are also few reports comparing atmospheric cooling in plains and basins. Based on such status, aims of the present study were set up.

CHAPTER II

METHODS OF OBSERVATIONS AND ACQUISITIONS OF DATA

2.1 Observations and acquisitions of data at Tsukuba

The data about wind, air temperature and heat balance components at the surface used in Chapter III were obtained using a real time data processor system for meteorological and hydrological measurements. This system belongs to the heat balance and water balance observation systems installed in the Hydro-Meteorological Observation Field of the Environmental Research Center (E. R. C.), University of Tsukuba, in the southwestern part of the Ibaraki Prefecture, Japan (Fig. 2.1).

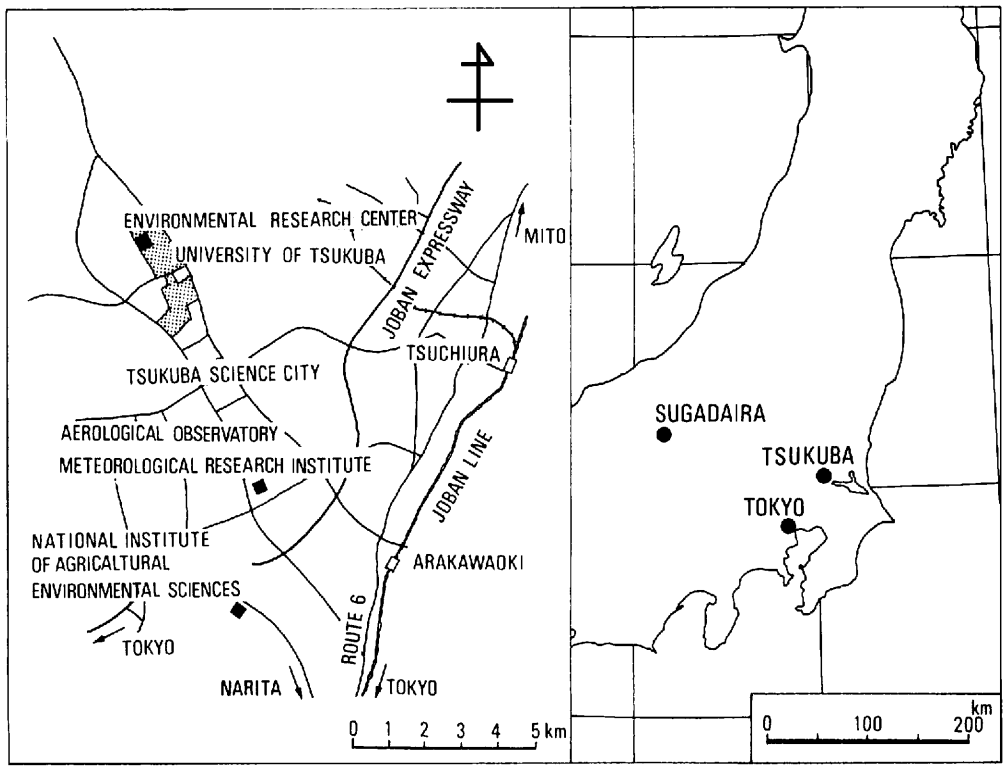

Fig. 2.1 Maps of Tsukuba.

The profiles of wind, air temperature and relative humidity were obtained from the Meteorological Research Institute (M. I. R.) which had a 200 m observation tower. This institute is located in the southern part of Tsukuba Science City. There are platforms and booms for meteorological instruments (anemometers, thermohygrometers and so on) at six heights (10, 25, 50, 100, 150 and 200 m above ground level) on the tower. Some radiative parameters (net radiation and upward and downward long-wave radiations) were obtained by the Aerological Observatory next door to the M. I. R.. Table 2.1 shows the observed parameters and instruments used at each observation site.

Aerological data used in calculation of the radiation terms were obtained from the Aerological Date

Table 2.1 The observed parameters and instruments used at each observation site.

(a) Environmental Research Center

parameter	instrument
air temperature	Pt resistance thermometer
wind direction	sonic anemometer SA-200
wind speed	sonic anemometer-thermometer PAT-311
net radiation	net radiometer (Middlton type) CN-11
sensible heat flux	sonic anemometer-thermometer PAT-311

(b) Meteorological Research Institute

parameter	instrument
air temperature	Pt resistance thermometer
wind direction	erovane type anemometer MV-110

(c) Aerological Observatory

parameter	instrument
net radiation	net radiometer CN-11
upward long-wave radiation	long-wave radiometer MS4R
downward long-wave radiation	long-wave radiometer MS4R

published by the Japan Meteorological Agency, and the spatial distributtion of wind, air temperature and duration of sunshine were obtained by the Automated Meteorological Data Acquisition System (AMeDAS).

2.2 Observations and acquisitions of data in Sugadaira

Data used in Chapter IV was obtained by field observations carried out in the Sugadaira Basin (Fig. 2.2). The basin, located 20 km southeast of Nagano City, has an elliptic shape with a 4 km long radius from northwest to southeast and a 1.5 km short radius from northeast to southwest, and 1,250 m above sea level in the central part of the bottom of basin.

The observations were made mainly in the central part of the bottom of the basin and the NE-facing slope of Mt. Omatsu on the south side of the basin. The top of this mountain is 1,648 m above sea level and the average inclination of the slope is approximately 9 degrees in the lower part and 25 degrees in the higher part of this slope. This slope was used as a skiing area in the winter. In the summer, the lower part of this slope was used for vegetable farms. The horizontal and vertical distributions of the wind and air temperature were observed at the bottom of the basin and on the slope. Fig. 2.3 shows the locations of the observation points and Table 2.2 show the observed parameters and instruments in the Sugadaira Basin. Moreover, the AMeDAS station whose data was used in Chapter V, is located at the north part of the bottom of the Sugadaira basin. This is pointed by the star in Figs. 2.2 and 2.3.

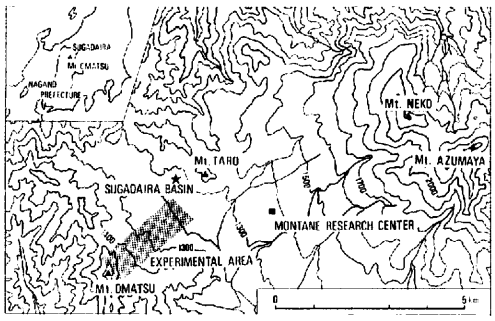

Fig. 2.2 A map of Sugadaira.
★: AMeDAS Observation point.

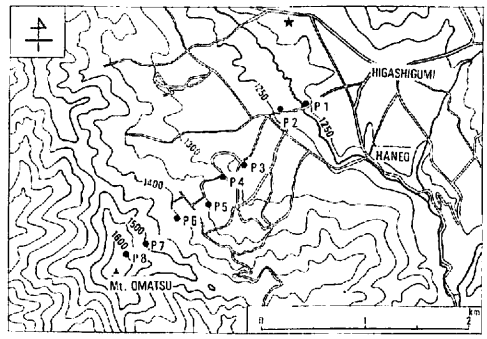

Fig. 2.3 Measurement sites (P1~P8) at the experimental slope in Sugadaira basin.
★: AMeDAS Observation point.

Table 2.2 The data periods and instrumentation in Sugadaira.

data period	parameter	instrument
May 6–10, 1982	air temperature	bimetal thermograph
		thermister thermometer
	wind direction	wind vane
	wind speed	three cup anemometer
	*vertical distribution	
	wind direction	tethered balloon
	wind speed	〃
	dry and wet air temperature	〃
Oct 3–4, 1982	air temperature	bimetal thermograph
June 10–12, 1984	air temperature	bimetal thermograph

CHAPTER III

STRUCTURES AND MECHANICS OF NOCTURNAL COOLING ON A PLAIN

3.1 Characteristics of nocturnal cooling on a plain

The change in air temperature in the nighttime, that is, the cooling rate *C. R.* is defined by the following equation;

$$C.\ R.\quad (\text{℃/h}) = \frac{T_s - T_r\,(\text{℃})}{h\,(\text{h})}\ , \tag{3.1}$$

where T_s (℃) represents air temperature at sunset, T_r (℃) at sunrise (hourly averaged values at 1.6 m high), and h (h) the duration time in hours.

The cooling rate depends on several factors. One of them is radiative cooling on the surface. In this chapter, the strength of radiative cooling on the surface is indicated by the integrated value of net radiation in the nighttime. Fig. 3.1 shows the definition of cooling rate and net radiation in the nighttime.

The seasonal variations of cooling rate, net radiation and wind speed at 1.6 m high at the E. R. C are shown in Fig. 3.2. Here, wind speed indicates the mean values and net radiation is the integrated values in the nighttime. In winter, the values of the cooling rate took a maximum value of about 0.5 ℃ and decreased gradually. After that they reached a minimum at about 0.2 ℃ in mid summer and then increased gradually. The values of net radiation were less than 0 W/m^2 and this indicates that the earth's surface lost heat through radiation in the nighttime. In winter, the absolute values of net radiation became large ranging from −40 to −50 W/m^2. Conversely, in summer, the values of net radiation ranged from −20 to −30 W/m^2. The values of wind speed in spring and summer were at least 1.0 m/s, and they are from 0.6 to 0.8 m/s in autumn and winter.

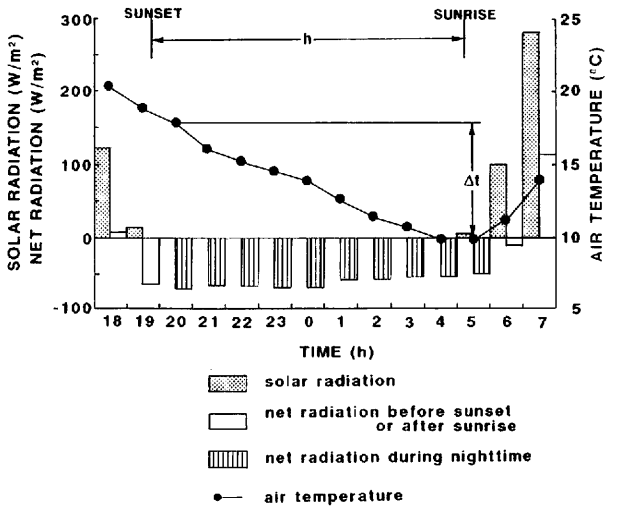

Fig. 3.1 The definition of cooling rate (observed at E.R.C. for May 21–22, 1986).

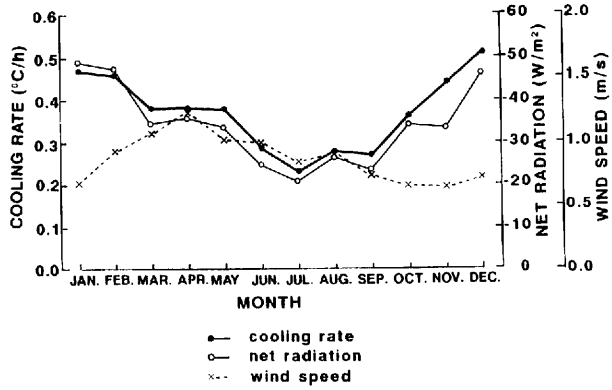

Fig. 3.2 The seasonal variations of cooling rate, net radiation and wind speed at 1.6 m high at the Environmental Research Center, University of Tsukuba for 1981–1987.

As shown in Fig. 3.2 the seasonal variation of net radiation was similar to that of cooling rate, but different from that of wind speed. Now, the relationships between cooling rate and meteorological components including net radiation and wind speed were analyzed statistically.

Table 3.1 shows the correlation coefficient between cooling rate and meteorological components containing net radiation on the surface, air temperature difference between 1.6 m and 12.3 m, wind speed at 1.6 m and 12.3 m and sensible heat flux at 1.6 m high. The high correlation coefficients in this table were found between cooling rate and net radiation (–0.69), and between cooling rate and air temperature difference (0.61). On the other hand, the correlation coefficients between cooling rate and wind speeds at two levels, and sensible heat flux were –0.32, –0.29 and –0.05, respectively. This indicates that when there was a large cooling rate in the nighttime, the radiative cooling on the surface was strong and the vertical distribution of air temperature became very stable near the surface. Moreover, when the wind was strong and mixed the air of the upper level and near the surface, it made the decrease of air temperature weak. Nishiyama (1985) reported that the correlation coefficient between the decreasing of temperature and accumulated values of net radiation at the ground surface from 1800 to 0700 was –0.53 at Tateno.

Table 3.1 The correlation between cooling rate and other meteorological components.

component	correlation coefficient
net radiation	–0.668*
wind speed (1.6 m)	–0.320*
wind speed (12.3 m)	–0.293*
sensible heat flux (1.6 m)	0.045
temperature gradient (1.6–12.3 m)	0.610*

*significant level 0.1 %

Then the dependence of net radiation on cooling rate is made more clear statistically. Fig. 3.3 shows the relationships of net radiation on the surface and cooling rate at 1.6 m high for various wind speeds. Fig. 3.3 (a) indicates the condition when the wind speed was in the range of 0.0 to 0.5 m/s, Fig. 3.3 (b) in the range of 0.5 to 1.0 m/s, Fig. 3.3 (c) in the range of 1.0 to 2.0 m/s, and Fig. 3.3 (d) for more than 2.0 m/s. Moreover, Table 3.2 shows the correlation coefficient, the ratio of cooling rate to net radiation, and the scatter of the points, regarding the statistical characteristics drawn in Fig. 3.3. As is clear from Fig. 3.3 and Table 3.2, the correlation between net radiation and cooling rate became weaker as wind speed increased. This indicates that cooling rate depended mostly on the strength of radiative cooling when the wind was weak. But the dependence of net radiation on the cooling rate became weaker as wind speed increased, because the strong wind was considered to make mechanical convective heating of air increase. Nishiyama (1985) reported that when the amount of net radiation was large, the cooling rate was sometimes small when the wind speed was high.

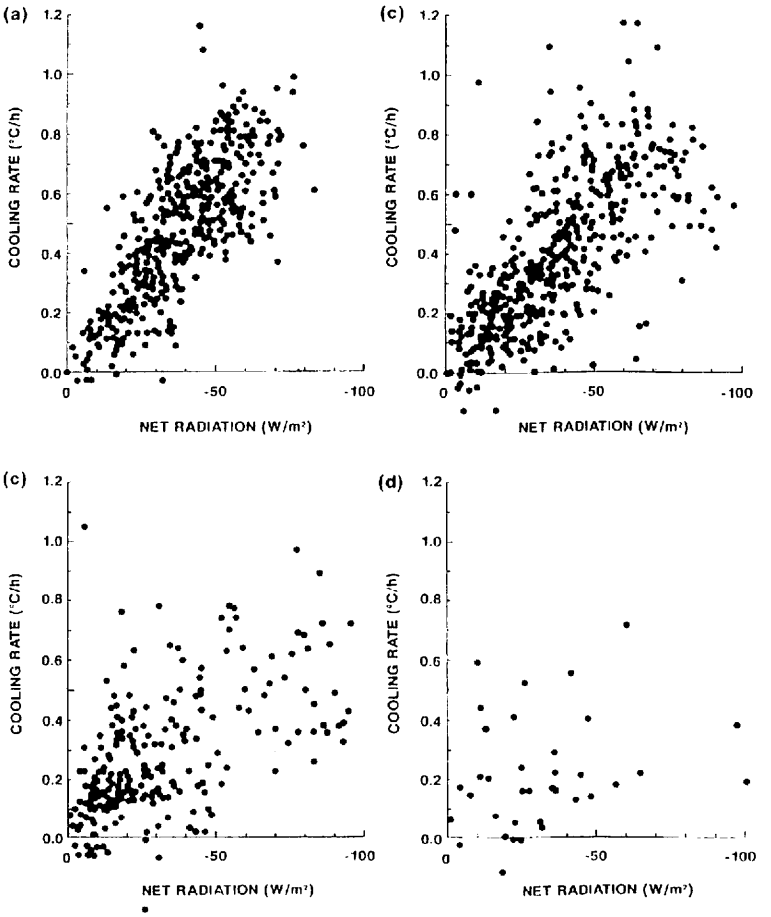

Fig. 3.3 The relationships of net radiation and cooling rate. Wind speed: (a) 0.0–0.5 (m/s), (b) 0.5–1.0 (m/s), (c) 1.0–2.0 (m/s) and (d) more than 2.0 (m/s).

Table 3.2 The relationships of net radiation and various wind speeds at 1.6 m.

(1)	(2)	(3)	(4)	(5)
0.0–0.5	416	-0.770*	-0.012	0.153
0.5–1.0	458	-0.699*	-0.010	0.185
1.0–2.0	228	-0.556*	-0.009	0.199
more than 2.0	36	-0.245	-0.007	0.210
total	1138	-0.669*	-0.011	0.193

* significant level 0.5 %

(1) wind speed (m/s)
(2) number of data
(3) correlation coefficient
(4) ratio of cooling rate to net radiation
(5) standard deviation

Net radiation in the nighttime, Rn, is expressed as follows:

$$Rn = L\downarrow + L\uparrow, \tag{3.2}$$

where, $L\downarrow$ is long-wave radiation from the air layer to the surface, that is, downward long-wave radiation, and $L\uparrow$ is long-wave radiation from the surface to the air layer, that is, upward long-wave radiation. Fig. 3.4 shows the relationships between net radiation, and downward and upward long-wave radiation. The

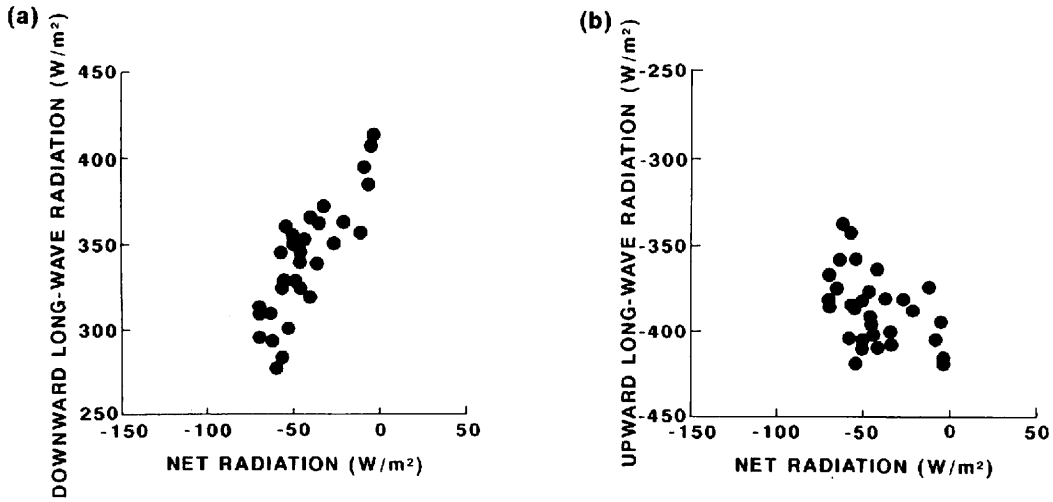

Fig. 3.4 The relationships between net radiation, and (a) downward and (b) upward long-wave radiations at E.R.C for May, 1982.

correlation coefficient between net radiation and downward long-wave radiation was 0.84 (significant level 0.1 %) and higher than that between net radiation and upward long-wave radiation. This indicated that the variation of net radiation mainly depended upon the variation of downward long-wave radiation in the nighttime.

Downward long-wave radiation on the surface was related to the amount of cloud cover and air temperature at upper levels. Fig. 3.5 shows the variations in the amount of cloud cover, downward long-wave radiation on the surface and air temperature at the 500, 600, 700, 800, 850, and 900 mb levels. The value of downward long-wave radiation was large when the value of the amount of cloud cover were high. This pointed out that clouds emitted radiation strongly and so they had strong effects on the value of downward long-wave radiation. Moreover, downward long-wave radiation changed almost in parallel with air temperature in the air layer between 800 and 900 mb levels, that is, between 1,000 and 2,000 m high above sea level. When the cold air flew into the air layer between 1,000 and 2,000 m level and decreased its temperature without clouds in the nighttime, amount of downward long-wave radiation reaching at the surface was small. As a result, radiative cooling at surface became strong, and the cooling rate became large.

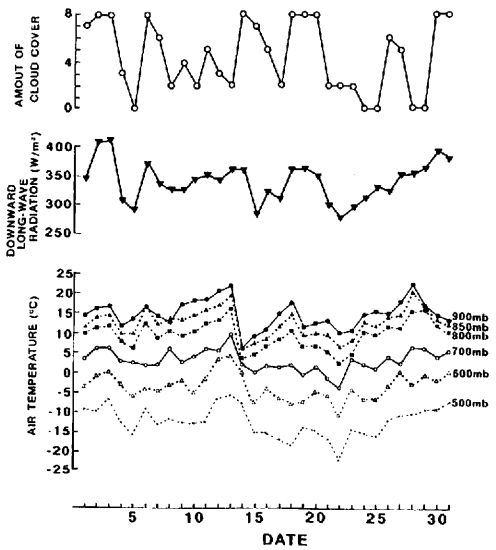

Fig. 3.5 Temporal variations of amount of cloud cover, downward long-wave radiation and air temperatures in the upper layer for May, 1982.

3.2 The structure of the surface inversion formed on a plain

As indicated in Chapter 3.1, the inversion layer near the earth's surface was formed when the cooling rate was large. In this analysis, the data used were obtained from the results observed at the 200 m high tower of the M. R. I. and at the observational field of the Aerological Observatory.

Fig. 3.6 shows the variations of surface and air temperatures at 1.6 m level and wind direction and speed at 10 m at nights on May 7–8 and 9–10, 1982, when cooling rate was large. The average values of wind speed at night were less than 1.5 m/s and wind direction was not fixed. Air and surface temperatures

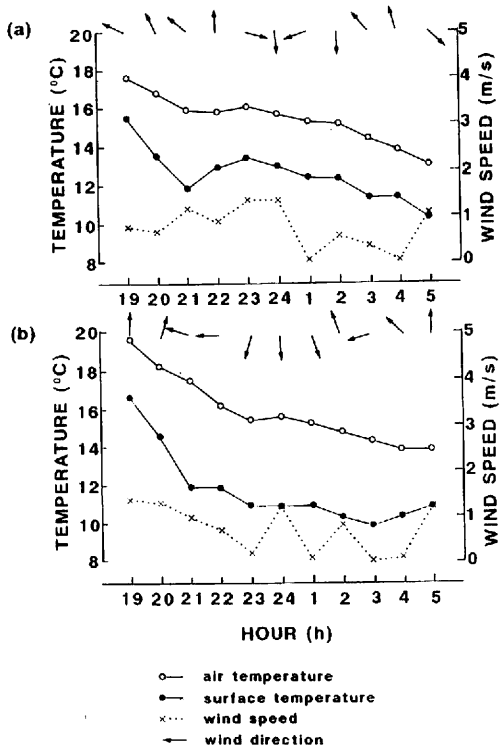

Fig. 3.6 Time variations of surface and air temperatures at 1.6 m high and wind direction and speed at 10 m high.
(a) May 7–8 and (b) May 9–10, 1982.

fell with time. But when wind speed became high from 2100 to 2400 on the 7th and from 2300 to 2400 on the 9th, air and surface tempertures were almost constant with time or rose a little. Moreover, surface temperature was 3–5 ℃ lower than air temperature all through the night.

Fig. 3.7 shows the variations of surface temperature and air tempertures at 7 heights, that is, 1.5, 10, 25, 50, 100, 150 and 200 m high above ground level. The decline of air temperature during the night became smaller with height. Air temperature at 200 m decreased by 1 or 2 ℃ and this value was 20–30 % as much as that near the surface. Air temperature droped in the same manner at three levels lower than 25 m.

Fig. 3.8 shows the variations of wind speed at the same 7 heights mentioned in Fig. 3.7. From sunset to midnight on the 9th, wind speed was high and reached values ranging from 5 to 8 m/s at higher levels. But after midnight, the wind speed deceased rapidly. Wind speed was less than 2 m/s at all heights around sunrise.

Figs. 3.9 and 3.10 show the vertical profiles of the air temperature, and the time and height sections of wind direction and wind speed in air layer between the surface and 200 m at night on May 7–8 and 9–10, 1982. Wind direction and wind speed are indicated by vector. Until midnight, wind speed was high and wind direction was almost fixed at all the levels between the surface and 200 m. But from midnight to early morning, wind speed was low and wind direction was variable. Wind direction at the two lower levels, 10 and 25 m, and at the three higher levels, 100, 150 and 200 m, were uniform, respectively. A surface

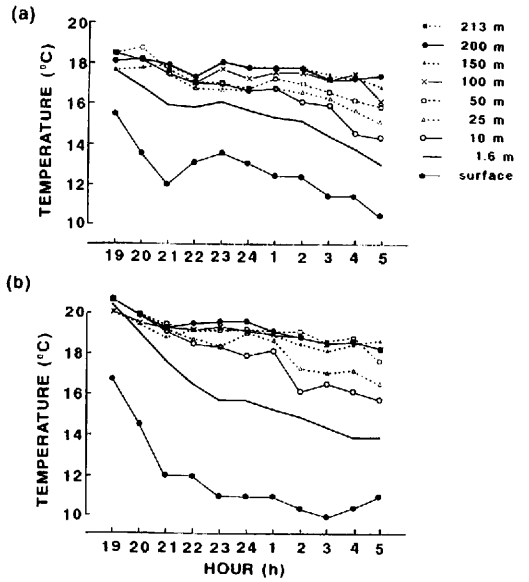

Fig. 3.7 Time variations of surface temperature and air temperatures at 7 heights.
(a) May 7–8 and (b) May 9–10, 1982.

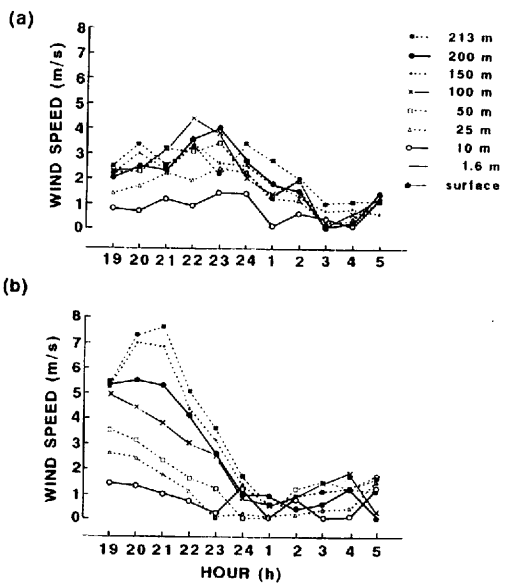

Fig. 3.8 Time variations of wind speed at 7 heights.
(a) May 7–8 and (b) May 9–10, 1982.

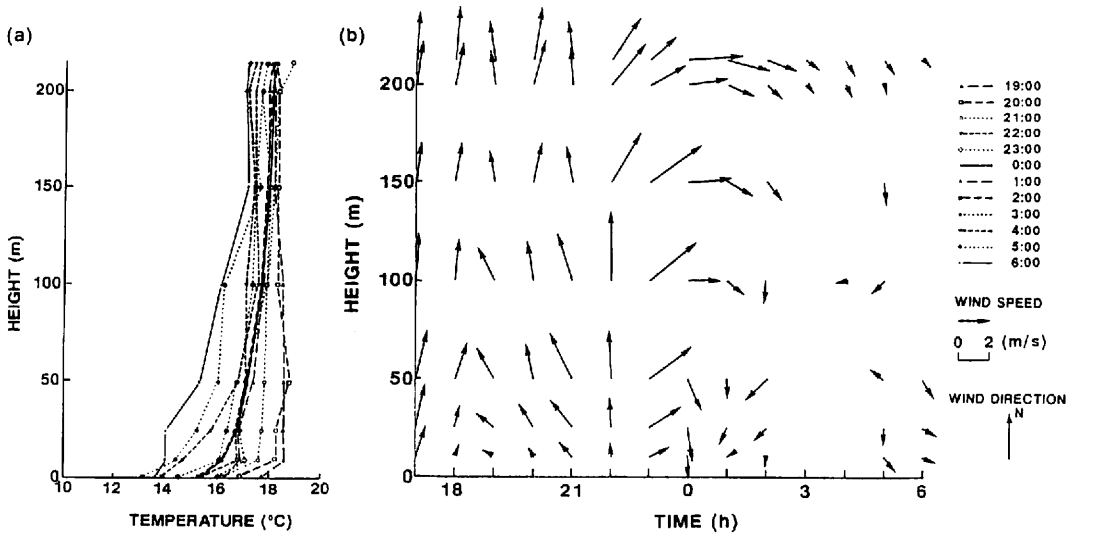

Fig. 3.9 Vertical profiles of the air temperature and time and height section of wind direction and speed on May 7–8, 1982.
(a) Vertical profiles and (b) time and height section.

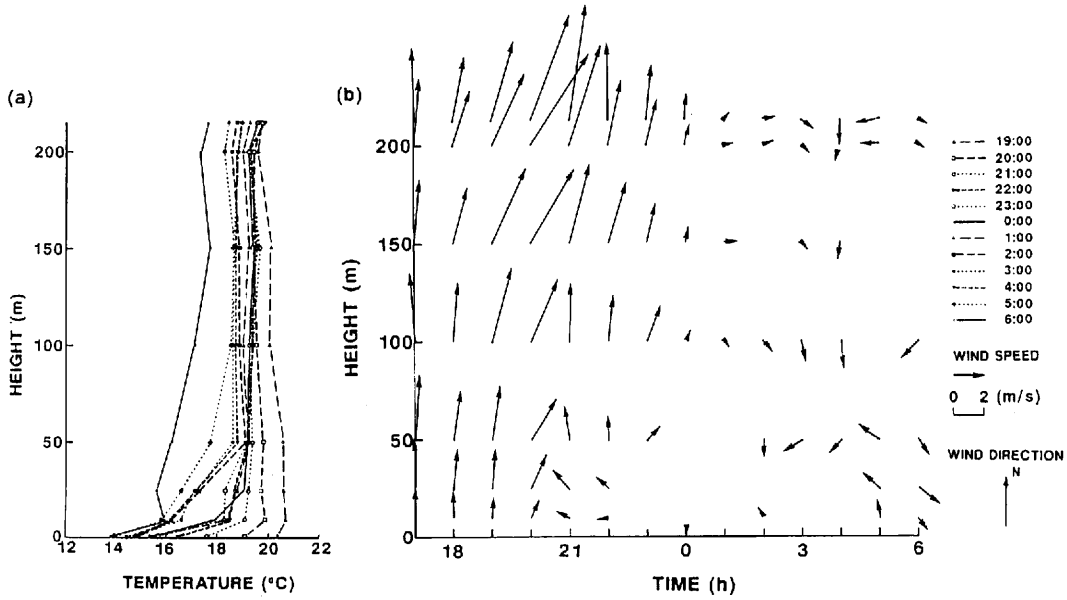

Fig. 3.10 Same as Fig. 3.9, but May 9–10, 1982.

inversion layer was formed between the surface and 100 m high, and air temperature gradient reached more than 3 ℃ in the air layer between the surface and a height of 10 m. A neutral layer or a weak inversion layer was formed in the air layer between 100 and 200 m.

The facts mentioned above suggested that the three sub-layers were distinguished in an air layer between the surface and 200 m high above sea level on the plain. The lowest sub-layer was the air layer between the surface and 25 m. In this layer, a strong inversion layer was formed and the wind direction at each level was uniform. The decrease of air temperature through the night was large, ranging from 3 to 4 ℃. This layer was definded as the lst sub-layer. The middle sub-layer was between 25 and 100 m. A weak inversion layer was formed and considered to be the transitional layer between the air layer formed on and near the surface, and that where general wind and synoptic-scale wind prevailed. This layer was defined as the 2nd sub-layer. The upper sub-layer was between 100 and 200 m with the small or zero air temperature gradient. The decrease of air temperature in this layer during the night was about half of that in the lst sub-layer, and the general and synoptic-scale wind prevailed in it. This layer was defined as the 3rd sub-layer.

3.3 Methods of analysis of variation of air temperature in the surface inversion layer formed in the nighttime

The time variation of air temperature in the air layer between a height of z_1 and z_2, in the nighttime when surface inversion layer is formed, and evapotranspiration is small enough to be neglected, expressed the following equation.

$$\left(\frac{\partial \theta}{\partial t}\right) = \left(\frac{\partial \theta}{\partial t}\right)_{Rn} + \left(\frac{\partial \theta}{\partial t}\right)_{TA}, \tag{3.3}$$

where, $\left(\frac{\partial \theta}{\partial t}\right)$ is the actual variation of air temperature in the air layer between the height z_1 and z_2,

$(\frac{\partial \theta}{\partial t})_{Rn}$ is the variation of air temperature by means of rediative balance in this air layer, $(\frac{\partial \theta}{\partial t})_{TA}$ by means of the advective and turbulent heat transfer.

To consider about time variation of air temperature in surface inversion layer mentioned chapter 3-2, each term in Eq. (3.3) was chosen as follows. On the term of the left side, $(\frac{\partial \theta}{\partial t})$, observed values were used. The first term of the right side $(\frac{\partial \theta}{\partial t})_{Rn}$ was calculated values using the following equation;

$$(\frac{\partial \theta}{\partial t})_{Rn} = -\frac{1}{C_p \rho (z_2 - z_1)} (Rn(z_2) - Rn(z_1)), \tag{3.4}$$

where, C_p was the specific heat of air at constant pressure, ρ the density of air, and z_1, z_2, the top and bottom of the air layer, and $Rn(z)$ net radiation flux at height z, respectively. The second term $(\frac{\partial \theta}{\partial t})_{TA}$ was the remainder.

In the nighttime, the net radiation flux at the height z can be expressed as follows.

$$Rn(z) = L\uparrow(z) - L\downarrow(z) \tag{3.5}$$

where, $L\uparrow$ is upward long-wave radiation and $L\downarrow$ downward long-wave radiation. Upward and downward long-wave radiation at any height were given by Katayama's equation (1972). The data used for calculating these long-wave radiations between the surface and 200 m level are ones obtained from the 200 m tower on the plain, and by the tethered balloon in the basin, respectively. And the data at the height over the 200 m level are obtained from the Aerological Data of Japan.

Table 3.3 shows the nights to consider time variation of air temperature when surface inversion layer was formed at Tsukuba. This place is representative of a place located on a plain. These selected nights were clear ones when the amount of cloud cover was less than 2/8.

Fig. 3.11 shows the comparison between measured and calculated values, and these values are the integrated ones of net radiation between 1900 and 0500 on the 7 nights mentioned in Table 3.3. The calculated values given by the equations mentioned above are found to be overestimated by about 7 %, but this overestimate is considered to be negligible in calculating time variation of air temperature due to radiation balance in the air layers.

The vertical distribution of net radiation obtained from the methods mentioned above is shown in Fig. 3.12. The gradients of net radiation was large in the air layer between the surface and 25 m high above ground surface, and this indicates that the drop of air temperature due to radiative balance was large, that is, radiative cooling was strong in this layer (see Eq. 3.2). Moreover, the gradients became small in accordance with height, and the difference of net radiation between at the surface and 200 m level was about 20 W/m^2.

Table 3.3 The days selected to consider variations of air temperature at night.

May	7 - 8, 1982
May	9 - 10, 1982
May	22 - 23, 1982
May	23 - 24, 1982
May	24 - 25, 1982
May	25 - 26, 1982
May	28 - 29, 1982

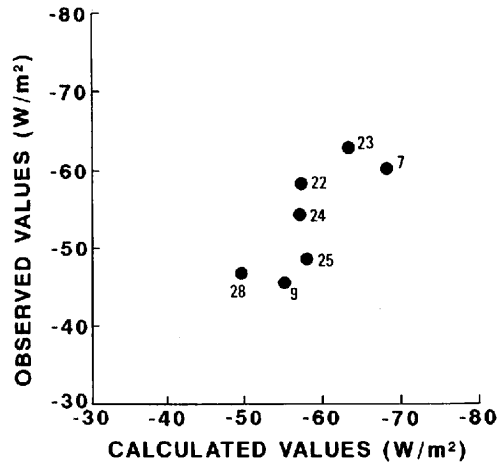

Fig. 3.11 The comparison between measured and calculated values of the integrated values of net radiation between 1900 and 0500 on 7 nights mentioned in Table 3.3.

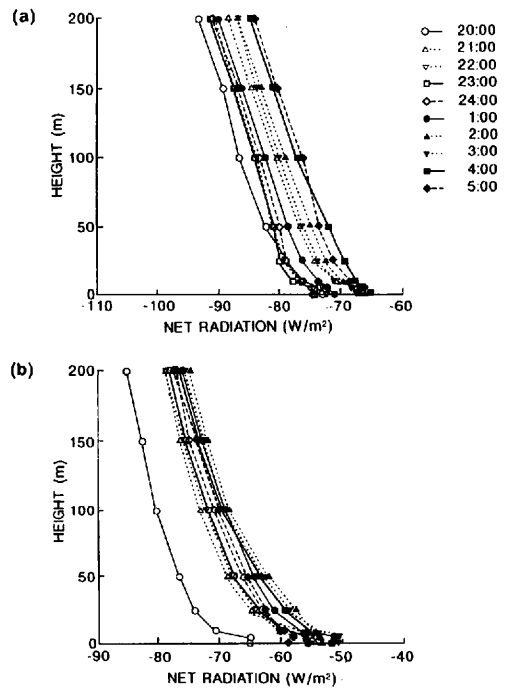

Fig. 3.12 Vertical distributions of net radiation obtained from the methods mentioned in Chapter 3.3. (a) May 7–8 and (b) May 9–10, 1982.

3.4 The atmospheric cooling in a surface inversion layer formed on a plain

As mentioned in chapters 3.1 and 3.2, in the air layer between the surface and 200 m high, the three sub-layers were distinguished by the differences in their structures. In this chapter, the actual variation of air temperature in each sub-layers was considered by the means shown in chapter 3.3. Fig.3.13 and 3.14 show the time variations of air temperature in three sub-layers on May 7–8 and 9–10.

The lst sub-layer was considered to be cooled by divergence of net radiation. This cooling was strong in early night, and air temperature fell at the rate of −0.5 to −1.0 ℃/h. But this cooling became weaker with time. Turbulent transfer and advection was considered to heat the lst sub-layer. On the occasion that air temperature rose slightly or was constant (from 2200 to 0200 on 7th, from 2300 on 9th to 0100 on 10th, and from 0200 to 0300 on 10th), these heating were relatively stronger than usual. The strength of the cooling due to divergence of net radiation in 2nd and 3rd sub-layers were about 1/3 as much as that in the lst sub-layer and almost constant through the night (−0.1 to −0.3 ℃/h). When air temperature in these sub-layers fell down at large rate (−0.4 to −1.0 ℃/h), turbulent transfer and advection cooled them. Conversely, when air temperature rose up, heating sub-layers due to turbulent transfer and advection was larger than radiative cooling.

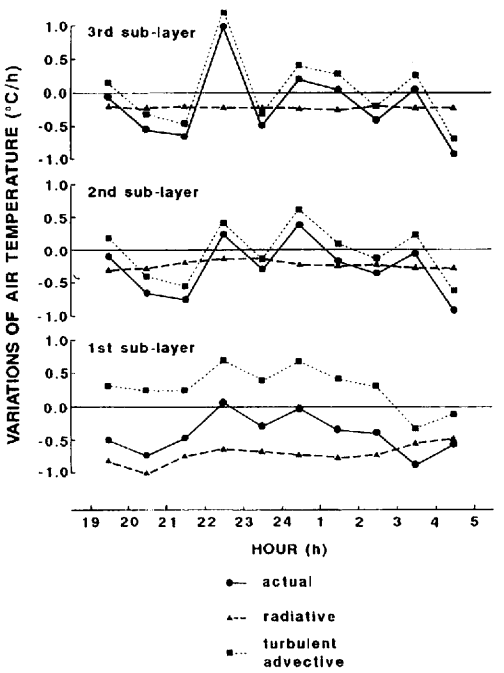

Fig. 3.13 Time variations of air temperature in the 1st, 2nd and 3rd sub-layers on a plain on May 7–8, 1982.

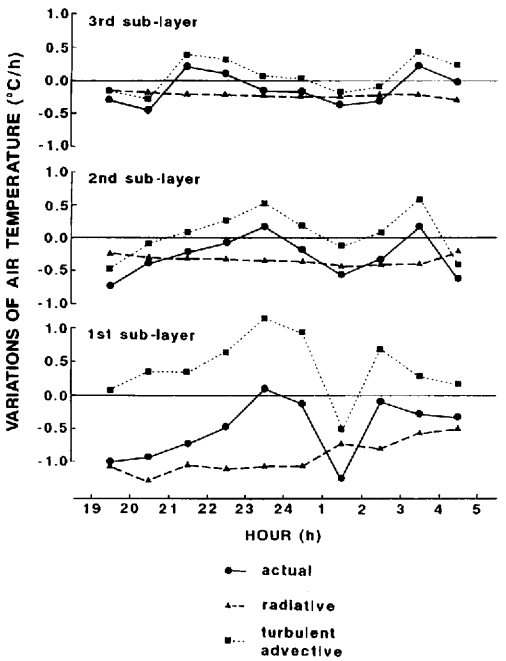

Fig. 3.14 Same as Fig. 3.13, but on May 9–10, 1982.

Fig. 3.15 shows the time variations of air temperature in the lst, 2nd and 3rd sub-layers throughout the night as shown in Table 3.3. The lst sub-layer was cooled in radiative process and heated by turbulent transfer and advection. On the other hand, air temperature in the 2nd and 3rd sub-layer fell down mainly due to radiative cooling, and sometimes additionally due to turbulent and advective cooling. Concerning to the air layer between the surface and 200 m high, in the same manner, air temperature fell down mainly due to divergence of net radiation, and sometimes additionally due to turbulence and advection. When the time variation of air temperature depended on radiative, turbulent and advective cooling, the drop in air temperature became larger than usual.

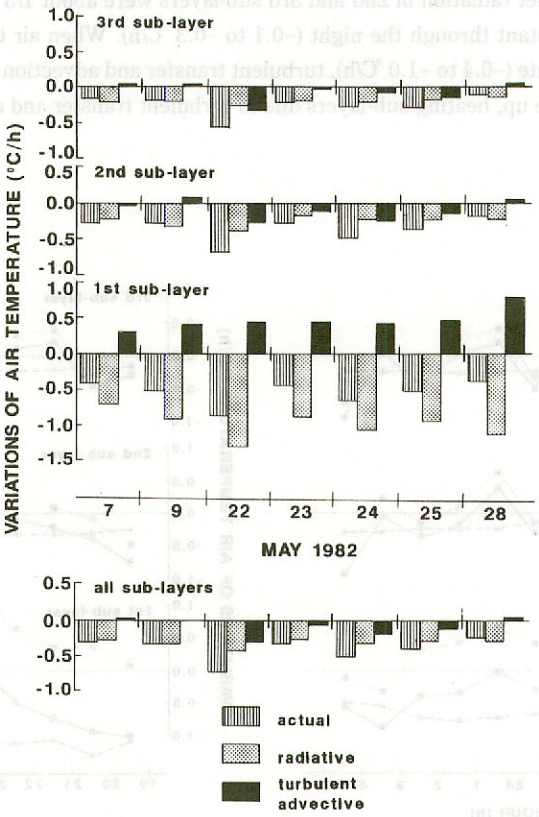

Fig. 3.15 Time variations of air temperature in the 1st, 2nd and 3rd sub-layers on a plain on 7 nights.

CHAPTER IV

STRUCTURES AND MECHANICS OF NOCTURNAL COOLING IN A BASIN

4.1 The structure of the surface inversion layer formed at the bottom of a basin

Analyses were made for the results observed in Sugadaira basin at two nights on May 7–8 and 9–10, 1982 when cooling rate was large. Fig. 4.1 indicates the time variations of wind and air temperature at the bottom of the basin. Air temperature dropped gradually and the wind speed became less than 0.5 m/s and is intermittent. This period was about 60–90 minutes long. When the wind increased except from 0030 to 0230 on the 9th, its direction is N, NNE, SW and WSW. These directions are consistent with the short axis of the basin. On the other hand, air temperature at the air layer between the surface level and the 200 m high above the bottom of the basin changed as shown in Fig. 4.2. Air temperature at the levels under 20–30 m high decreased gradually. But at the levels from 30 to 90 m, air temperature changed remarkably, and rose especially at midnight (2400 on May 7 and 0100 on May 10). Air temperature at the levels over 100 m was about constant or decreased a little through the night.

Fig. 4.3 and 4.4 show the vertical profiles of air temperature and the time and height sections of wind

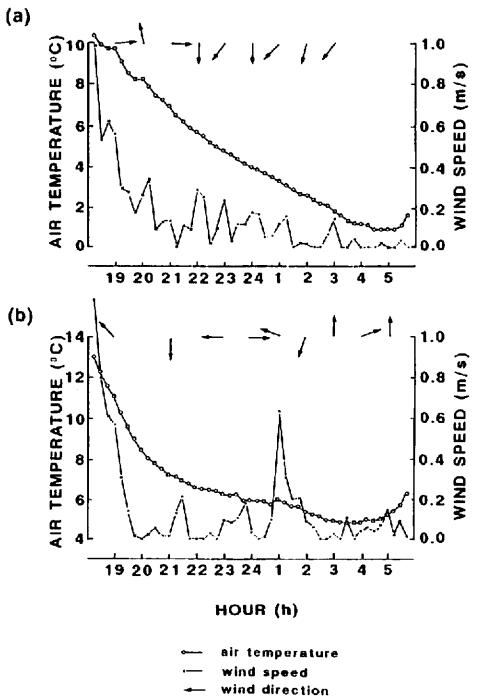

Fig. 4.1 Time variations of wind and air temperature at the bottom of the basin.
(a) May 7–8 and (b) May 9–10,1982.

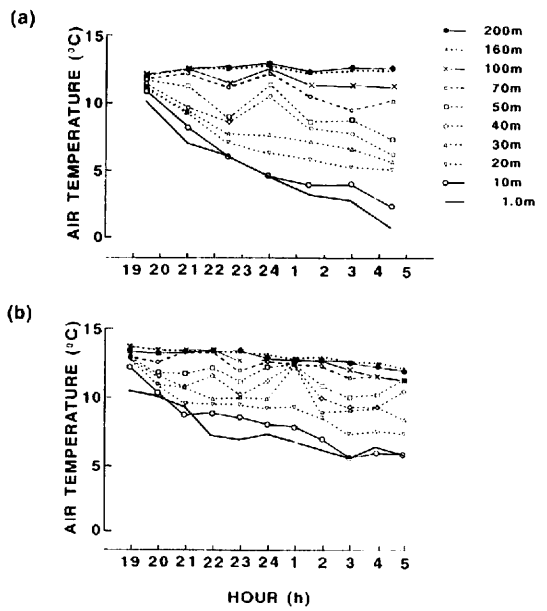

Fig. 4.2 Time variations of air temperature above the bottom of the basin.
(a) May 7–8 and (b) May 9–10,1982.

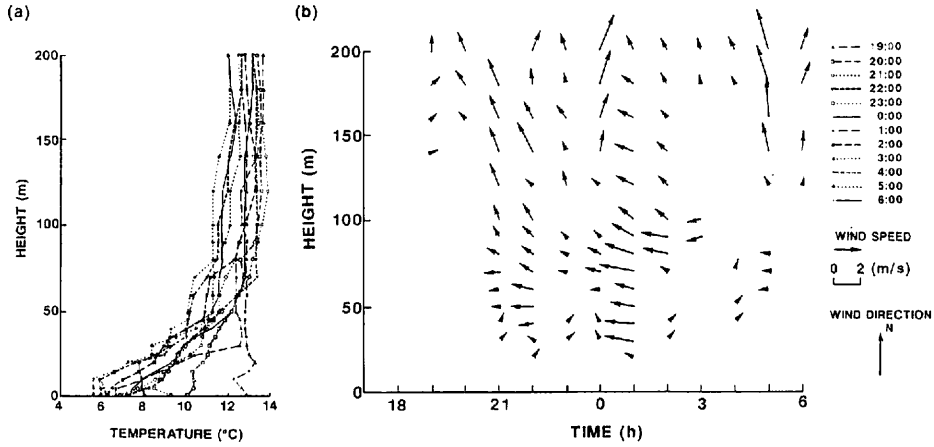

Fig. 4.3 Vertical profiles of air temperature and time and height sections of wind direction and speed above the bottom of the basin on May 7–8, 1982.
(a) Vertical profiles and (b) time and height section.

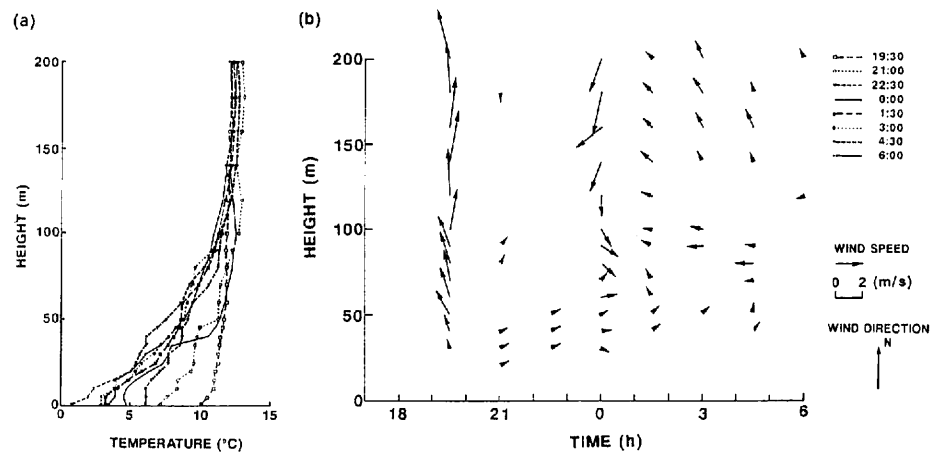

Fig. 4.4 Same as Fig. 4.3, but on May 9–10,1982.

direction and speed above the bottom of the basin. The wind directions and speeds are indicated by vectors as shown in Fig.3.9 and 3.10. After sunset, the inversion layer was formed above the bottom of the basin, and especially in the air layer under 30–40 m high, air temperature gradient was very steep. The height of the inversion layer reached 70–100 m high, and was about 1/2 of the relative height of the surrounding ridges. Also, the difference of air temperature between this height and the bottom of the basin reached 7–12 ℃. At the levels under 30–40 m high, wind speed was less than 0.5 m/s or there was no wind except at midnight.At the levels between 30 and 50 m, a gentle wind with WSW-SW direction blew. At the levels between 40 to 100 m, there was a prevailing E-ESE wind, and this direction was in parallel to the long axis of the bottom of the basin. When the general wind became strong and invaded into the basin, air temperature rose at the levels above 30–40 m, and the thickness of the strong inversion layer fell down to a range of 25–40 m high above the bottom of the basin. But in the air layer less than 30–40 m, the air was

continuously cooled with time, and wind whose direction was different from the general wind flew or it was completely calm.

It has definitely shown by the time variations of wind and air temperature in the basin at nights when cooling rate was large, that three sub-layers were distinguished in the air layer above the bottom of a basin. The lowest sub-layer was thermally stable, and the wind direction was along the short axis of the basin with a velocity of less than 0.5 m/s. Air temperature in this sub-layer decreased gradually during the night (the air layer from the surface to 30–40 m high). The middle sub-layer was also stable condition but at midnight the air temperature rose temporarily (from 30–40 to 70–80 m high). The upper sub-layer was almost neutral condition and the meso-scale wind prevailed and air temperature in this layer was almost constant or decreased a little through the night (form 70–80 to 200 m high). These sub-layers were called the 1st, 2nd and 3rd sub-layer, respectively. Moreover, the 1st and 2nd sub-layers were equivalent to cold air lake.

4.2 The structure of the surface inversion layer formed on a slope

Fig. 4.5 shows the time variations in air temperature at the observation points located at the bottom of the basin and on the slope of Mt. Omatsu on May 7–8 and 9–10, 1982, respectively. Air temperature at the

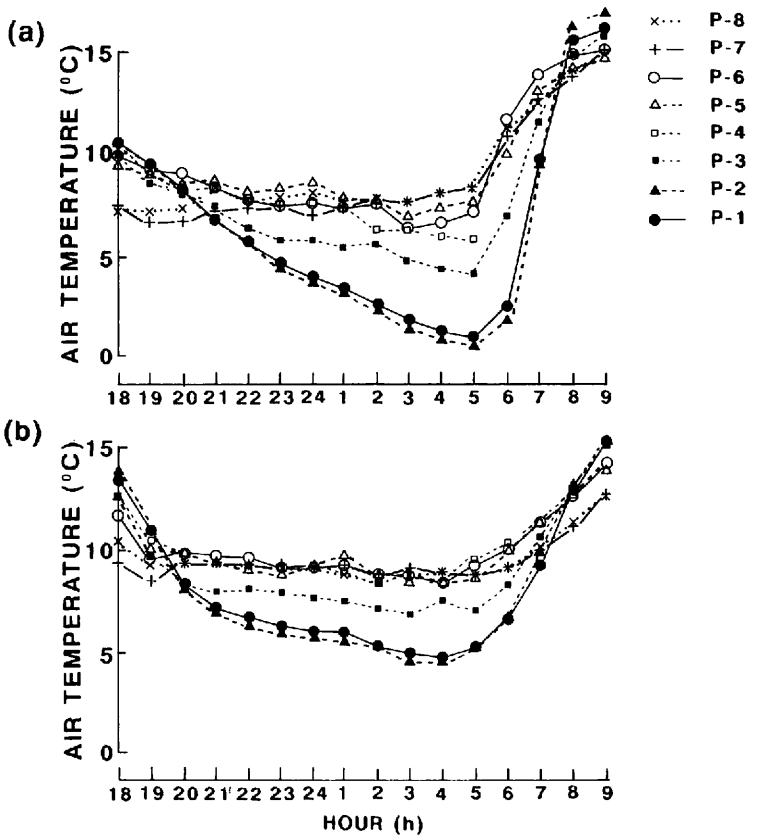

Fig. 4.5 Time variations of air temperature at the bottom of the basin and on the slope of Mt. Omatsu.
(a) May 7–8 and (b) May 9–10,1982.

observation points at the bottom of the basin (P-1 and P-2) fell steadily with time until the minimum air temperature occurred in the basin. Conversely, air temperature at the stations on the low and middle parts of the slope (P-3, low part; P-4, P-5, and P-6, middle part of the slope) decreased a little all through the night. Air temperature on the high part of the slope (P-7 and P-8) was almost constant with time. In this way, air temperature at the bottom of the basin became lower than those on the middle and high parts of the slope. The place on the slope where air temperature is higher than at the bottom of the basin is called the thermal belt (Geiger, 1965; Yoshino, 1975, 1986). At the time when minimum air temperature occurred at the bottom of the basin, the difference of air temperature between at the middle part of the slope and at the bottom of the basin, reached almost 5–7 ℃.

The time variation and its distributtion of air temperature on the slope of Mt. Omatsu will be considered further in detail. The distributions of air temperature at the bottom of the basin and on the slope of Mt. Omatsu for the nights are shown in Fig. 4.6 through 4.9. These figures show the isoplethes of air temperature at the bottom of the basin and on the slope. Fig. 4.6 shows the period from 1800 on 7 to 0900 on 8 May, 1982, Fig. 4.7 from 1800 on 9 to 0900 on 10 May, 1982, Fig. 4.8 from 1800 on 3 to 0700 on 4 Oct., 1982 and Fig. 4.9 from 1800 on 9 to 0700 on 10 June, 1984. It is thought that they represent typical distributions of air temperature at clear nights in spring, summer and autumn. Air temperature, at the observation points located at the bottom of the basin (1,250 m above sea level) and at less than 1,300 m on the slope, fell with time until the minimum air temperature occurred in the basin. Conversely, air temperature at the points higher than 1,300 m on the slope decreased only a little during the night. When the minimum air temperature occurred, the difference of air temperature between at the points higher than 1,300 m on the slope and at the bottom of the basin reached almost 5–7 ℃.

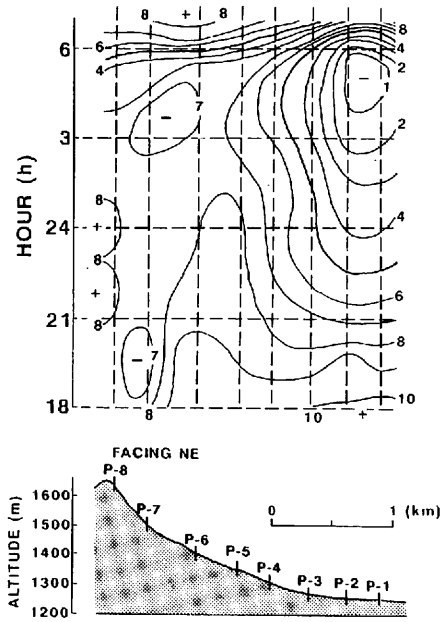

Fig. 4.6 Isopleth of air temperature at the bottom of the basin and on the slope of Mt. Omatsu from 1800 May 7 to 0700 May 8, 1982.

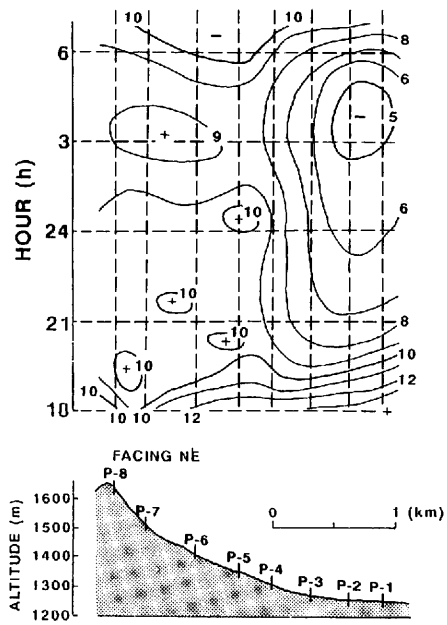

Fig. 4.7 Same as Fig. 4.6, but from 1800 May 9 to 0700 May 10, 1982.

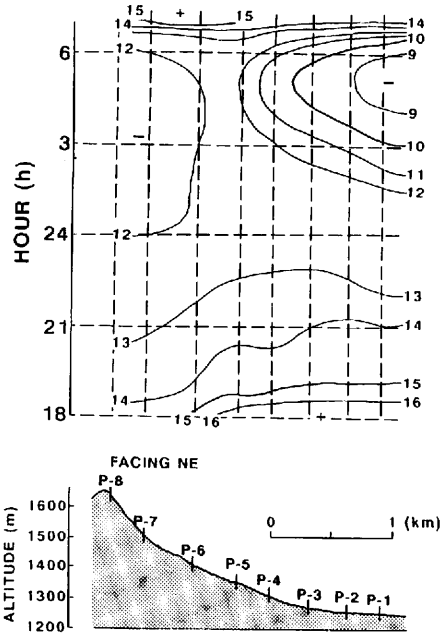

Fig. 4.8 Same as Fig. 4.6, but from 1800 Oct. 3 to 0700 Oct. 4, 1982.

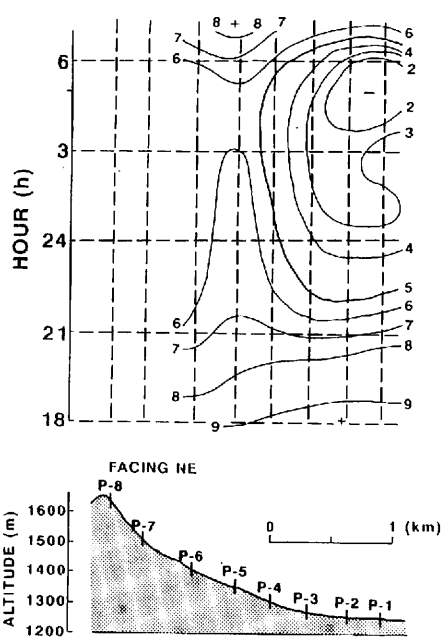

Fig. 4.9 Same as Fig. 4.6, but from 1800 June 11 to 0700 June 12, 1984.

Fig. 4.10 shows the variation in wind direction and speed and temperature at the observation point P-5 from 7 to 8 and 9 to 10 May, 1982. As mentioned above, the point P-5 (1,320 m) is representative of the observation points on the slope. After the sunset, wind direction was W-SW and it coincided with the direction of cold air drainage formed on the slope. Wind speed fluctuated periodically in the range of 0 to 3 m/s. On the other hand, air temperature dropped down with fluctuation in the range of 1 to 2 ℃, and the amount of decrease in air temperature during the night was 3-4 ℃. This value was 1/3-1/2 of it observed at the bottom of the basin from sunset to sunrise.

Concerning the relationships of the variations and fluctuations between wind speed and air temperature, air temperature often dropped down when the wind speed was high mentioned above. Nakamura (1976) and Yoshino, *et al.* (1981) reported that when cold air drainage flows on the slope, the relationship between the time variations of wind speed and air temperature was negatively correlated. The facts revealed here confirm the same relationships.

The time variations of air temperature above the surface up to 100 m high on the slope at the night are given in Fig. 4.11. The time variation of air temperature was the largest near the surface and became small with height. The features of the variation of air temperature at the levels from the surface to 10 m were different from those 10 m to 100 m. Though air temperature at the levels from 10 m to 100 m rose from 2100 to 2230 on the 7th, 2100 to 2200 on the 9th and 0300 to 0400 on the 10th, air temperature fell continuously near the surface. But from 2230 to 2400 on the 7th, and from 2300 to 2400 on the 9th, air temperature rose near the surface and at the levels higher than 10 m.

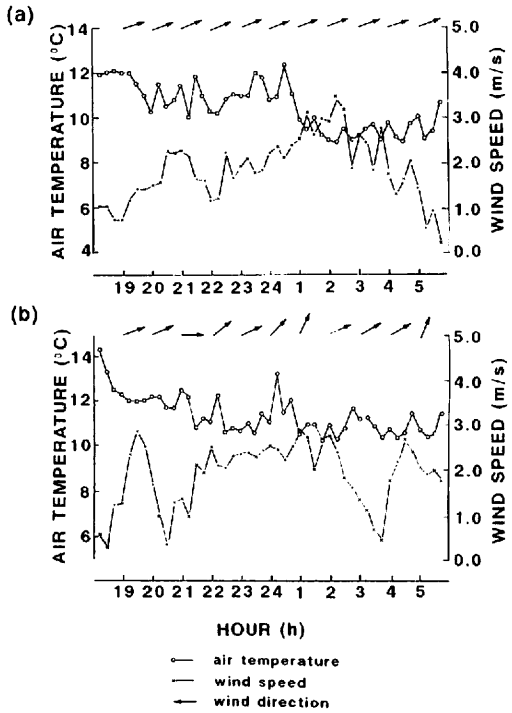

Fig 4.10 Time variations of air temperature and wind speed on the slope of Mt. Omatsu. (a) May 7–8 and (b) May 9–10, 1982.

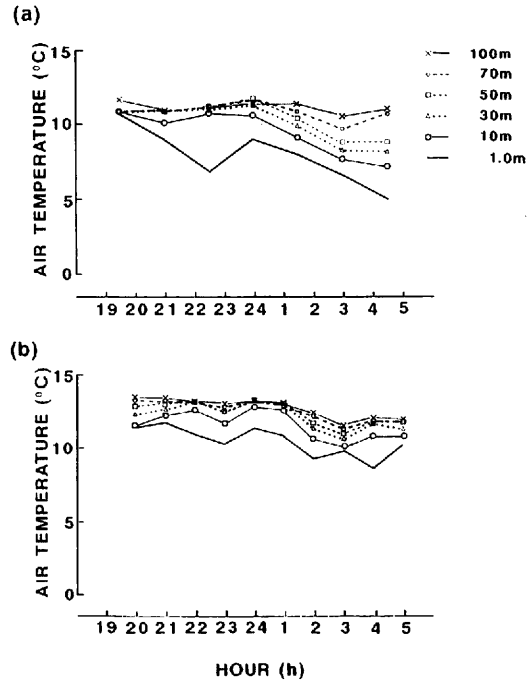

Fig. 4.11 Time variations of air temperature on and above the slope. (a) May 7–8 and (b) May 9–10, 1982.

Fig. 4.12 shows the vertical profiles of air temperature above the surface on a slope. Air temperature gradient differed remarkably between above and under 10 m high; larger under this level, smaller or about zero above it.

As mentioned above, it can be generalized that air temperature at the bottom of the basin fell continuously during the night, but conversely it fluctuated on the slope. Air temperature dropped down when the wind speed is high. Secondly, it is striking that the two sub-layers were distinguishable on the slope. The 1st sub-layer was characterized by the air layer from the surface to 10 m high with the large air temperature gradient. The 2nd sub-layer (the air layer from 10 m to 100 m high) had smaller air temperature gradient than the 1st sub-layer.

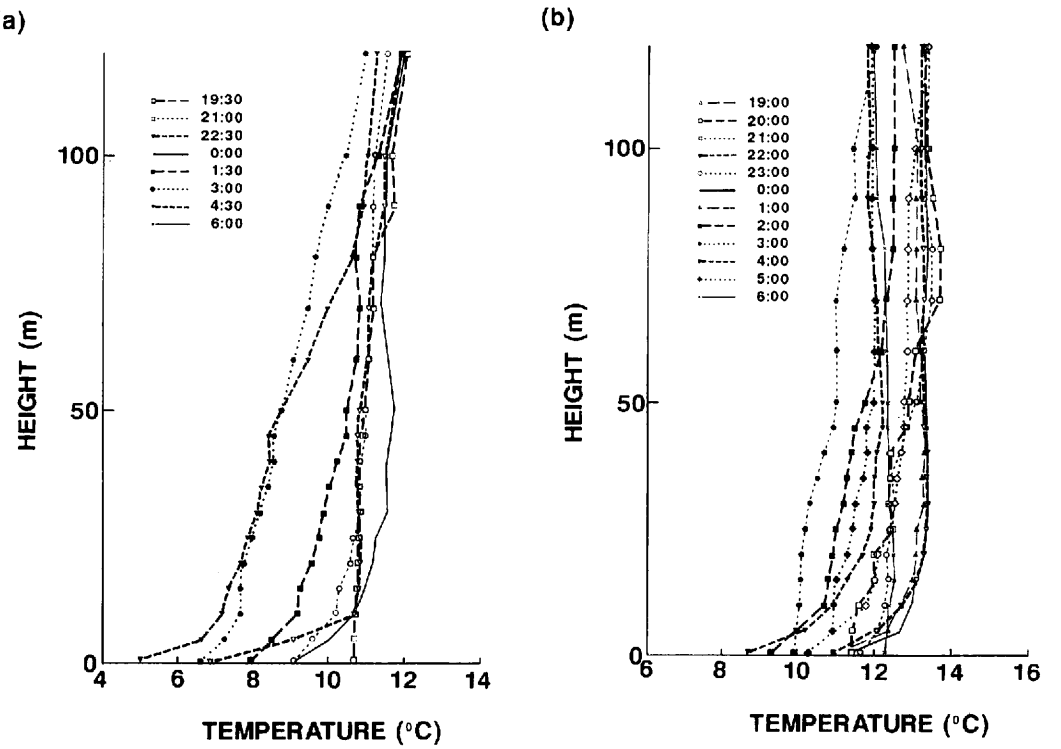

Fig. 4.12 Vertical profiles of air temperature on and above the slope.
(a) May 7–8 and (b) May 9–10, 1982.

4.3 The atmospheric cooling in a cold air lake and cold air drainage formed distinguishable in a basin

As mentioned in Chapters 4.1 and 4.2, three sub-layers and two sub-layers were distinguishable in the basin and on the slope when the inversion layer was formed, respectively. In this chapter, time variation of air temperature due to radiative process, turbulent transfer and advection in the respective sub-layers were estimated by the method mentioned in Chapter 3.3.

At first, the vertical distribution of net radiation was calculated by Katayama's formula (1974). In the basin area, the effects of the slope's characters on calculating radiation components were considered to be negligible, because the angle of the slopes was generally 5–6 dergrees and the effects of the slopes with

such angles were less than 5 W/m^2 by Kondo (1982). Fig. 4.13 shows the vertical distribution of net radiation in an air layer between the ground surface and at a height of 200 m in the nighttime on May 7-8 and 9-10, 1982. The difference of net radiation between at the surface to 200 m levels reached about 25 W/m^2, and this indicated that the rediative cooling at the basin was about 1.2 times stronger than at the plain. Based on this distribution, the time variation of air temperature due to radiation balance was calculated.

Figs. 4.14 and 4.15 show the time variations of air temperature in these three sub-layers at the nights on May 7-8 and 9-10, 1982. The 1st sub-layer was cooled due to divergence of net radiation, turbulent transfer and advection of cold air. The radiative cooling was almost constant or slightly weak with time (at the rate of -0.4 to -0.9 ℃/h). Turbulent and advective cooling were large early evening (more than 1.0 ℃/h), so the air temperature dropped down rapidly. In midnight or early morning, turbulent and advective heating occurred, and so air temperature in 1st sub-layer dropped down slightly or rose up. The strength

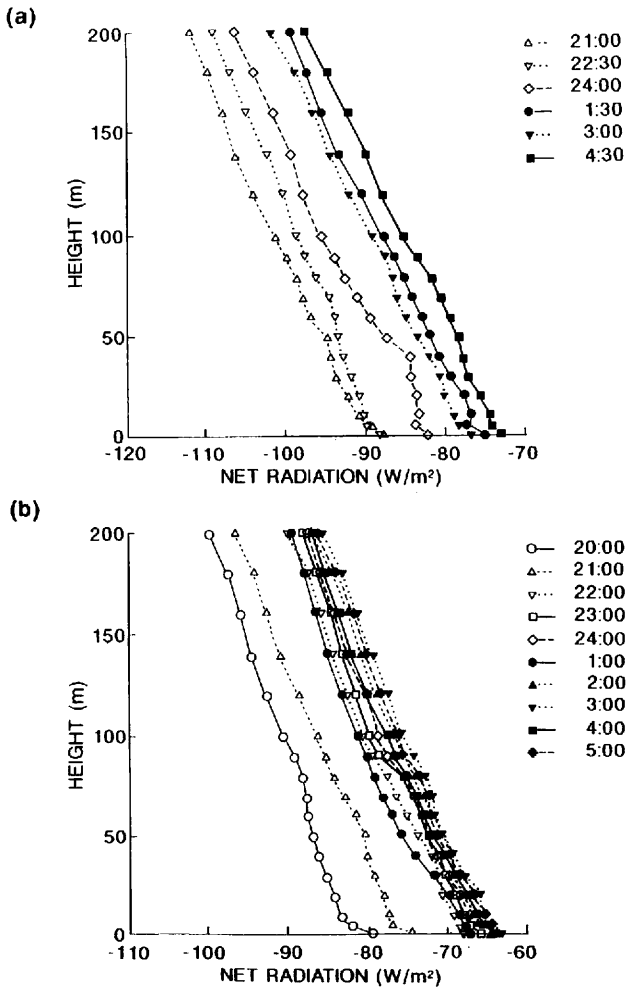

Fig. 4.13 Vertical distributions of net radiation in the air layer between the ground surface and at a height of 200 m at the nights on May 7–8 and 9–10, 1982.

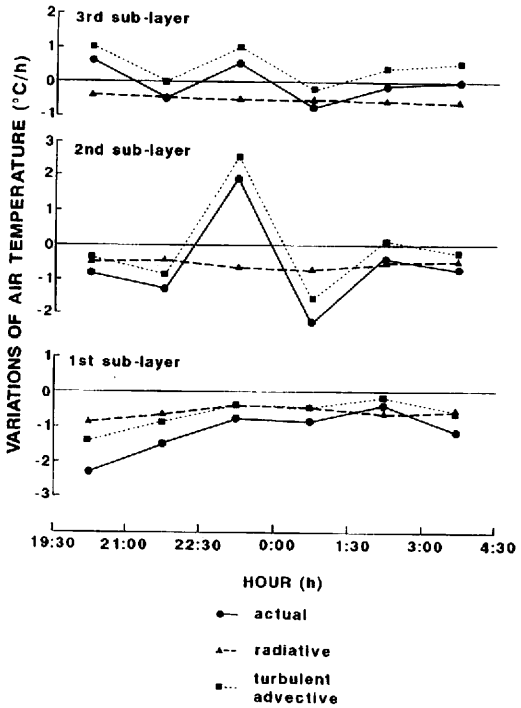

Fig. 4.14 Time variations of air temperature in the three sub-layers at the night on May 7–8, 1982.

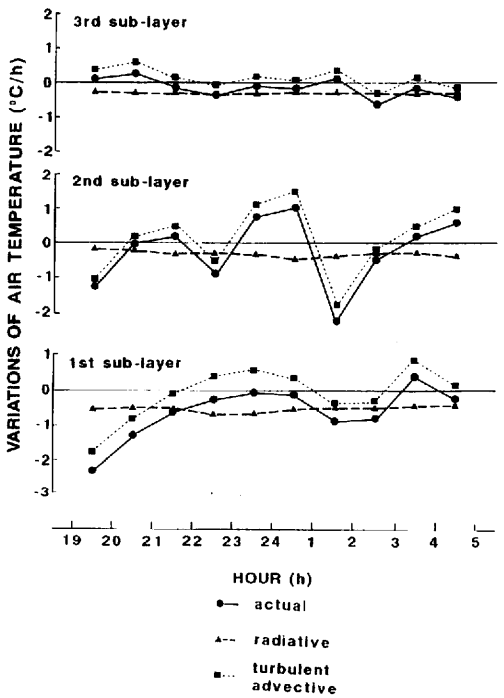

Fig. 4.15 Same as Fig. 4.14 but at the night on May 9–10, 1982.

of radiative cooling in 2nd and 3rd sub-layers were almost constant (0.2 to 0.5℃/h). Early evening in 3rd sub-layer and midnight in 2nd or 3rd sub-layers, turbulent and advective heating occurred, and air temperature rose up rapidly. At this time, wind speed was high as mentioned in Chapter 4.2, and it is considered that turbulent convection became active, and that warm air advected from upper air layer to these sub-layers and heated them. After the strong heating due to turbulence and advection ended, the air temperature in 2nd sub-layer fell down. Moreover, the scale of time change of air temperature was found to become smaller with height.

Figs. 4.16 and 4.17 show the time variations of air temperature above the slope on May 7-8 and 9-10. The strength of radiative cooling in the 1st sub-layer was almost constant through the night (-1.2 to -1.5 ℃/h). Only when wind speed became strong above the basin, and strong turbulent and advective heating occurred, air temperature rose up. Except above time, air temperature in the 1st sub-layer dropped down mainly due to radiative cooling (-0.5 to -1.2 ℃/h). The strength of radiative cooling in the 2nd sub-layer was about 0.3 ℃/h and constant through out the night. When turbulent convection occurred and warm air

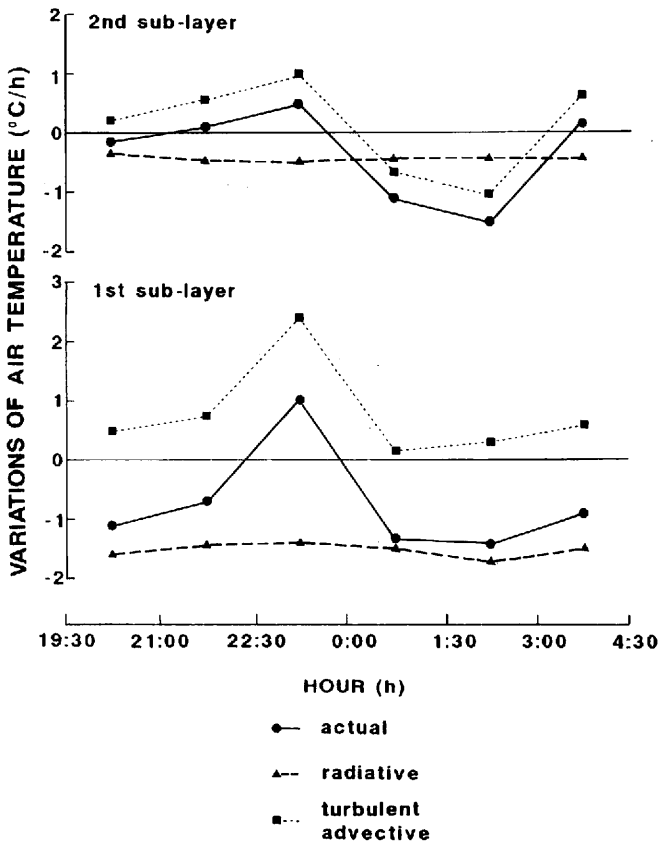

Fig. 4.16 Time variations of air temperature in the air layer between the ground surface and 100 m level above the slope at the night on May 7-8, 1982.

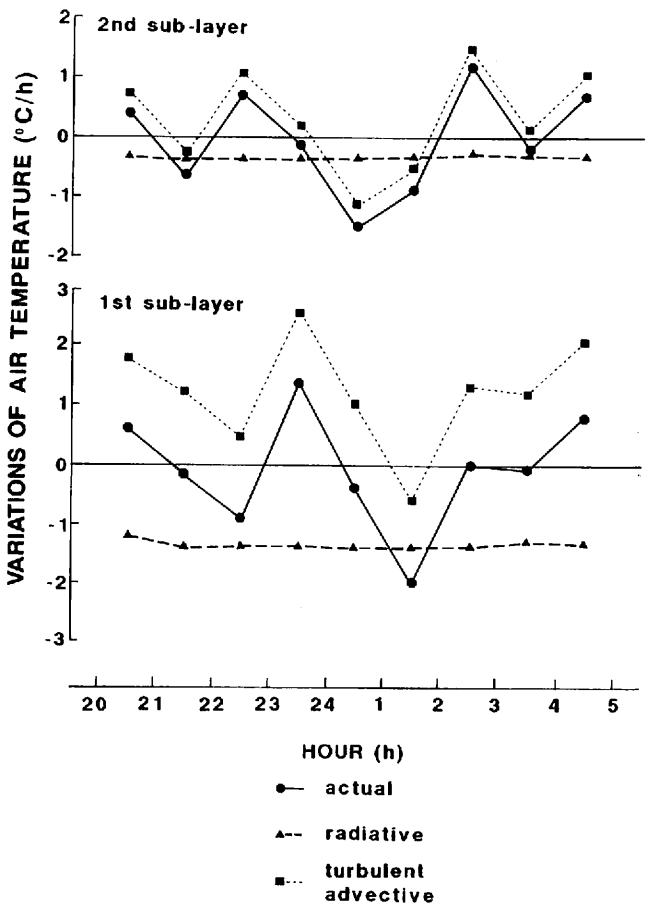

Fig. 4.17 Same as Fig. 4.16, but at the night on May 9–10, 1982.

advected into this sub-layer, air temperature rose up. Conversely, when turbulent and advective cooling occurred, that is, cold air advected into this air-layer, air temperature fell down.

Fig. 4.18 shows the nocturnal mean of the variations of air temperature in the air layer from the surface to 200 m high in the basin and from the surface to 100 m high on the slope, on May 7-8 and 9-10. In the 1st sub-layer, air temperature decreased due to radiative, turbulent and advective cooling. But the 2nd and 3rd sub-layers were cooled due to radiative cooling, and heated due to turbulence and advection. Moreover, considering the air layer from the surface to 200 m high, the air temperature was found to change only due to radiative cooling (about −0.5 ℃/h). On the other hand, air temperature on and above the slope at night changed due to radiative cooling and advective heating. Furthermore, radiative cooling and advective heating in 1st air-layer on the slope were stronger than any other air-layer in the basin and on the slope. This is firstly because the divergence of net radiation was large by higher surface temperature in contrast with the bottom of the basin, and by the effects of the height of ground surface above sea level, and secondly because cold air drainage flowing down away on the slope carried cold air formed on it.

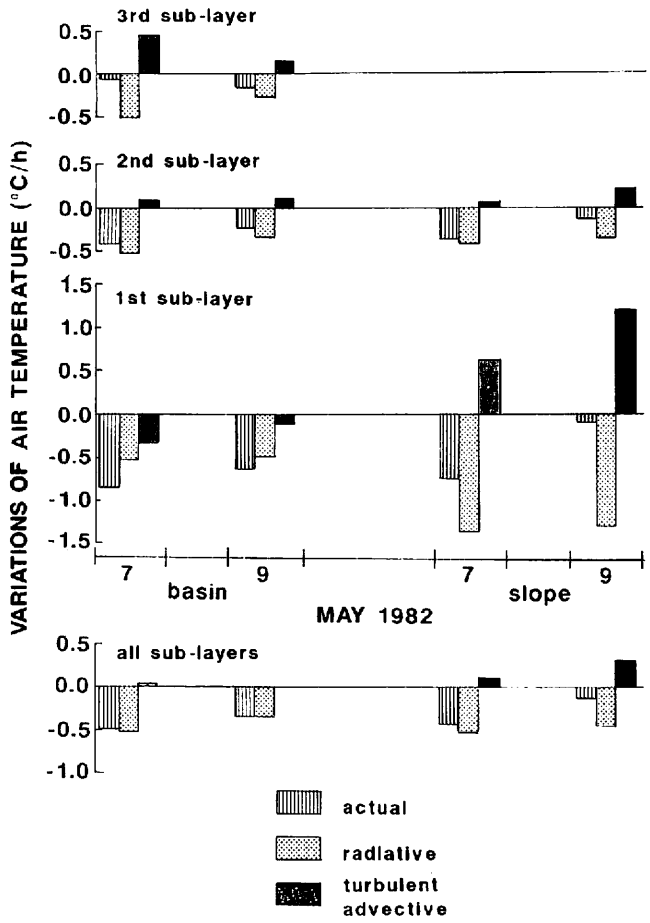

Fig. 4.18 The nocturnal mean of the variations of air temperature in the air layer from the surface to 200 m high at the bottom of the basin and from the surface to 100 m high on the slope on May 7–8 and 9–10, 1982.

4.4 The atmospheric circulation and cooling when cold air lake and cold air drainage are formed in the basin

In Chapters 4.1 and 4.2, the characteristics of surface inversion layer formed in the basin and cold air drainage flowing on the surrounding slope were clarified. Here, the relationships of the two are dealt with.

Figs. 4.19 and 4.20 shows the time variations of wind and potential temperature in the basin and on the slope. The arrows denote the wind direction and speed observed in the basin. After sunset, potential temperature dropped down in the air layer under 70 m high above the bottom of the basin and lower part of the slope (below 1,300 m above sea level). The potential temperature in the air layer between 20 and 40 m coincided with that on the middle part of the slope (from 1,300 to 1,400 m), and the wind direction in the air layer between 30 and 40 m (in 1st sub-layer) indicated the existence of the advection from the slope. On the other hand, cold air drainage flew down intermittently with its speed of more than 2.0 m/s on the slope. About midnight, the wind flowing in upper air layer became stronger temporally and potential

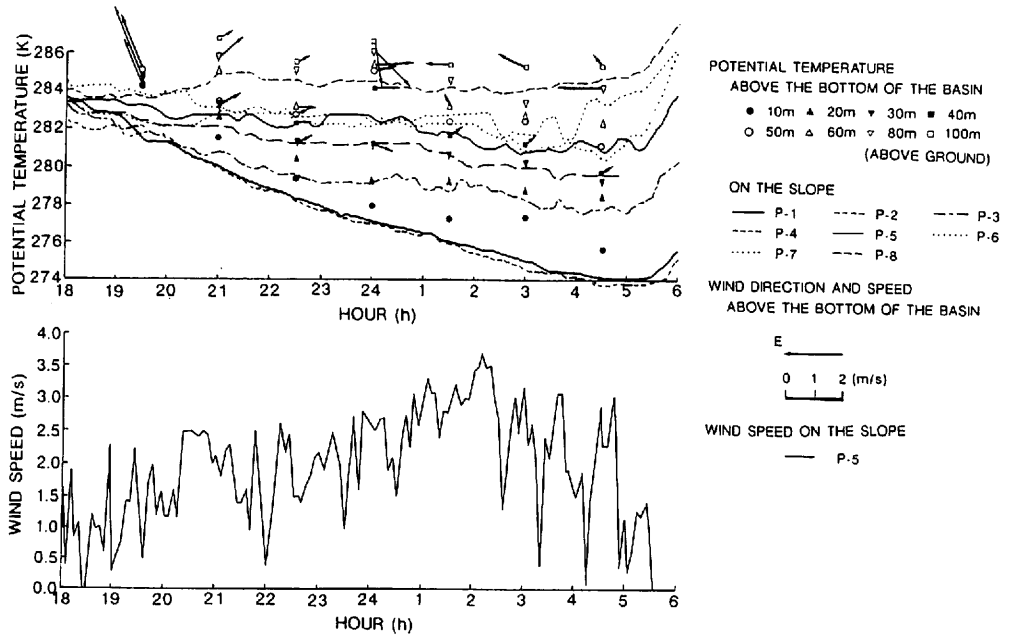

Fig. 4.19 Time variations of wind and potential temperature above the bottom of the basin and on and above the slope at the night on May 7–8, 1982. The arrows denote the wind direction and speed observed above the bottom of the basin.

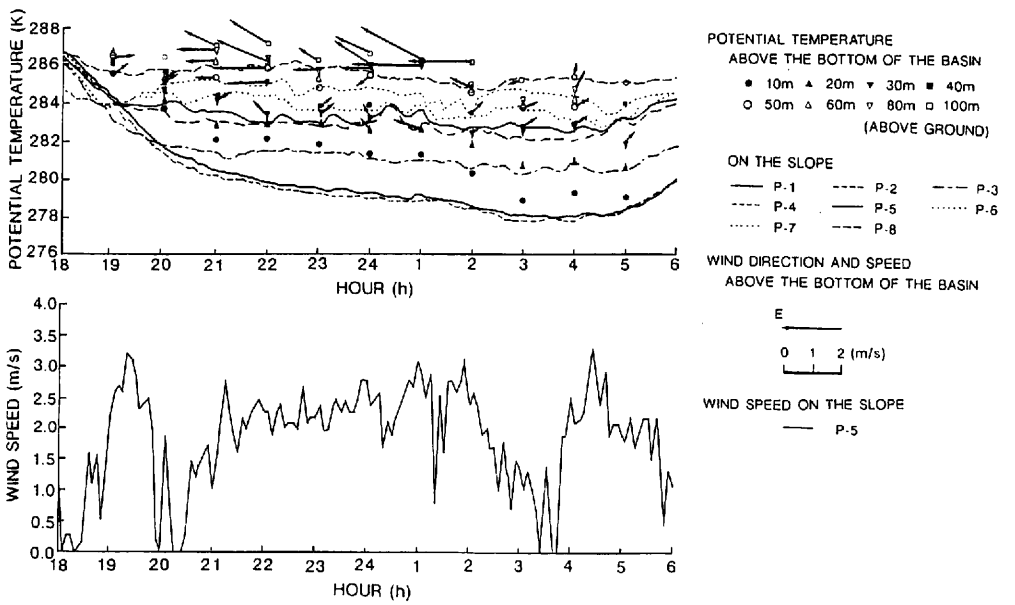

Fig. 4.20 Same as Fig. 4.19, but at the night on May 9–10, 1982.

temperature rose in the air layer over 30–40 m high above the bottom of the basin. After that, the wind became weak and potential temperature dropped down in the air layer between 40 and 60 m above the bottom of the basin (in 2nd sub-layer), and as a result, this temperature was equal to that on the middle part of the slope. The wind direction indicated the existence of the advection from the slope. On the slope, the wind speed was 2–3 m/s and cold air drainage flew down on it.

From the time variations of wind and potential temperature mentioned above, it was found that the nights on May 7-8 and 9-10 were divided into the three stages as follows:

(1) The first stage was the period from sunset to the midnight when air temperature and potential temperature fell down in the basin.

(2) The second stage was the period when the wind flowing in the upper air layer became strong. A rise in air temperature and potential temperature occurred in the basin and on the slope.

(3) The third stage was the period when the wind became weak again and air temperature and potential temperature dropped down.

Here, to make clear the relationships between cold air lake formed above the bottom of the basin and cold air drainage flowing on the slope in each stage, vertical cross sections of potential temperature are shown in Figs. 4.21 through 4.23.

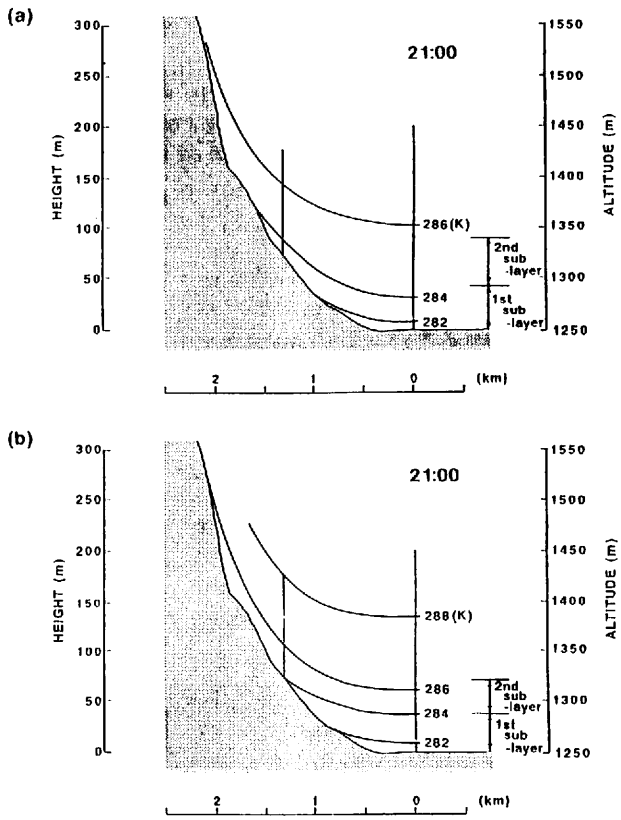

Fig. 4.21 Vertical cross sections of potential temperature at the first stage. (a) May 7–8 and (b) May 9–10, 1982.

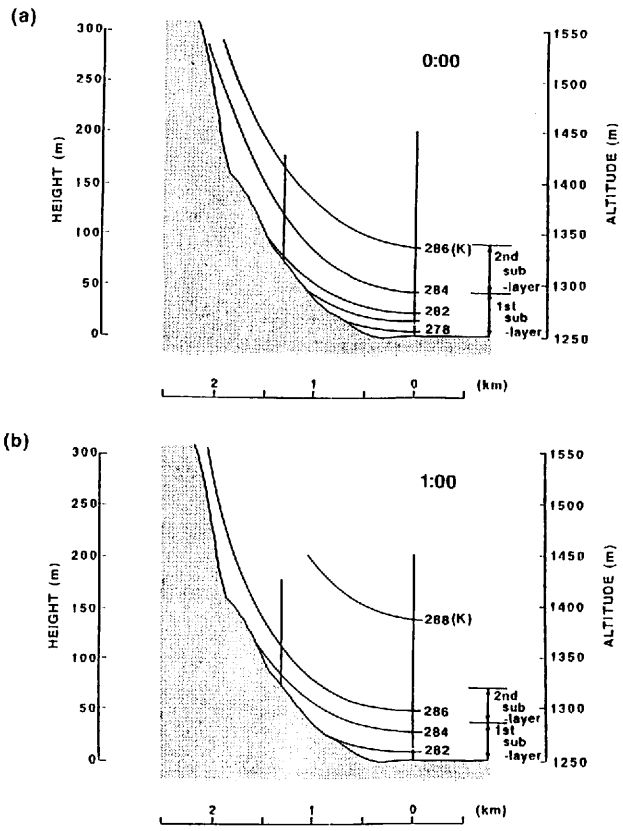

Fig. 4.22 Same as Fig. 4.21, but at the second stage.

In the first stage (at 2100 on May 7 and 9), the isopleth line was horizontal above the bottom of the basin and dense from the surface to 80–100 m high. The isopleth line became a downward convex curve with approaching the surface of the slope. This indicates that at the same height above sea level, the potential temperature on the slope was lower than that above the bottom of the basin, and a result of this, cold air drainage formed on the slope (Fleagle, 1950; Petkovšek and Hočevar, 1971; Sahashi, 1974). The cold air formed on the middle part of the slope flew into the air layer above the bottom of the basin along with the isopleth line of the potential temperature, and this fact was made sure by the field observation in the Moshiri Basin, Hokkaido (Magono *et al.*, 1982). From the results shown in Figs. 4.19 and 4.20, cold air drainage advected into the air layer from the surface to 20–50 m level above the bottom of the basin, that is, the 1st and 2nd sub-layers (in cold air lake).

In the second stage (at 2400 on May 7 and 0100 on 10), the potential temperature in the air layer under 40 m high above the bottom of the basin was the same as that near the surface on the middle part of slope. But the wind direction did not agree with the direction of air flow advected from the slope, so cold air formed on the middle part of the slope did not flow into this air layer.

In the third stage (at 0430 on May 8 and 0400 on 10), the minimum air temperature occurred at the bottom of the basin. The potential temperature in the air layer over 40 m level above the bottom of the basin was the same as that near the surface on the middle part of slope. Moreover, weak wind with WSW-SW

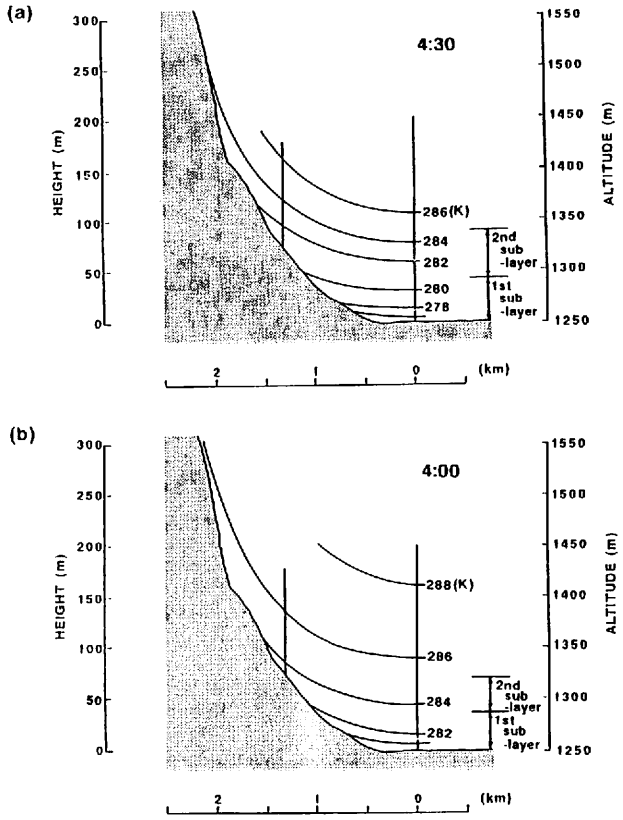

Fig. 4.23 Same as Fig. 4.21, at the third stage.

flew above 40 m high (shown in Figs. 4.19 and 4.20), So the cold air drainage formed on the middle part of slope was considered to flow into this air layer, that is, the 2nd sub-layer.

Fig. 4.24 shows the variation of air temperature above the bottom of the basin in each stage on the May 7–8 and 9–10. In the first stage, the 1st sub-layer and 2nd sub-layer cooled rapidly due to radiative, turbulent and advective cooling. 50–70 % of the actual cooling in the 1st sub-layer and 30–70 % in the 2nd were accounted for by turbulent and advective cooling. In this stage, cold air formed on the middle part of the slope flew into the 1st and 2nd sub-layer, so this turbulent and advective cooling was considered to be caused by the inflow of this cold air drainage. The air temperature in the 3rd sub-layer was about constant with time or rose up.

In the second stage, the wind speed in the 2nd sub-layer increased by the strengthening of the wind in upper air layer, and air temperature rose due to turbulent and advective heating. But air temperature dropped down gradually, mainly due to the radiative cooling in the 1st sub-layer.

In the third stage, air temperature in the 1st sub-layer dropped down mainly due to radiative cooling, because potential temperature in the 1st sub-layer was lower than that on the middle of the slope, so cold air drainage was not able to flow into it. In the 2nd sub-layer, 30–40 % of the actual cooling was due to the turbulence and advection because of cold air drainage advected from the surrounding slopes.

As mentioned above, it is considered that cold air drainage flowing on the middle part of the slope

contributed to the time variation of air temperature in the surface inversion layer air layer formed above the bottom of the basin, that is, cold air lake.

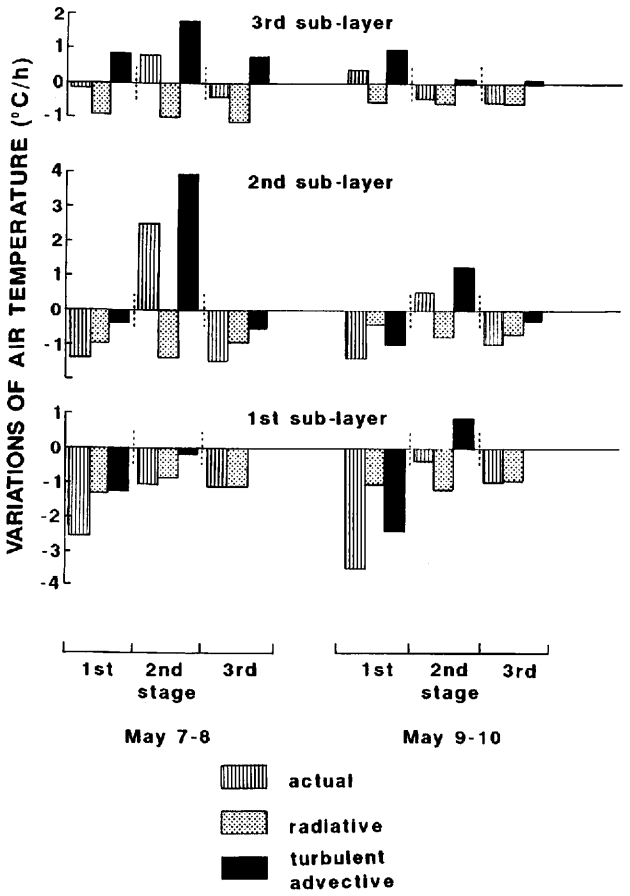

Fig. 4.24 The variations of air temperature above the bottom of the basin in each stage on the May 7-8 and 9-10, 1982.

CHAPTER V

GEOGRAPHICAL CHARACTERISTICS OF NOCTURNAL COOLING

5.1 The characteristics of nocturnal cooling in the Kanto District

As mentioned in Chapter III, in Tsukuba located in the Kanto Plain, time variation of air temperature in surface inversion layer during the night mainly depended on the radiative cooling, and turbulent and advective heating when wind speed was strong. In this chapter, the characteristics of spatial distribution of variation of air temperature in Kanto Plain were dealt with.

At first, the spatial distribution of the cooling rate in the Kanto District is given. Fig. 5.1 shows the observation points in the Kanto District used in this analysis. The observation points are distributed almost without exception in the Kanto District and the distance between each point is about 20 km on average. Data used in this analysis are hourly averaged values of wind direction and speed, air temperature and duration of sunshine in May, 1986.

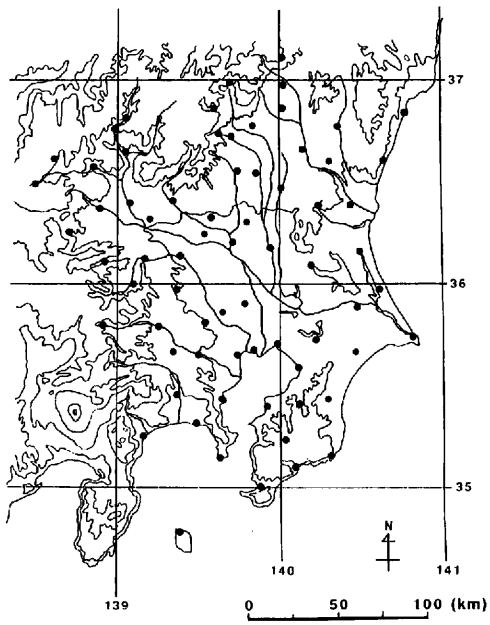

Fig. 5.1 Observation points of the AMeDAS in the Kanto Plain.

Fig. 5.2 shows the spatial distribution oh the average monthly cooling rate for May 1986 in the Kanto District. Here, the cooling rate is defined by the following equation (see in Chapter 3.1);

$$C.R.\ (\text{℃/h}) = \frac{T_s - T_r\,(\text{℃})}{h\,(\text{h})}, \tag{5.1}$$

where *C. R.* (℃/h) represents the cooling rate, T_s (℃) the air temperature at sunset (2000), T_r (℃) the air temperature at sunrise (0500), and h (h) is the duration time in hours (10 hours). The cooling rate was more than 0.3 ℃/h in the inland area of the Kanto District, and was more than 0.4 ℃/h in the Minakami, Numata, Nakanojo and Chichibu Basins. On the other hand, it was less than 0.2 ℃/h along the Pacific coastline.

Fig. 5.3 shows the spatial distribution of the monthly wind direction of the highest frequency and the average monthly wind speed during the night (between 2000 and 0500). Here, wind direction is indicated by arrows and wind speed is indicated by isoplethes. In the western part of Kanto District, a wind direction of N-W prevailed, and in the eastern part, a wind direction of N-E prevailed. In Oshima, Miura Peninsula and the southern part of Boso peninsula a wind direction of SW prevailed. On the other hand, in Chichibu, Numata, Nakanojo and Daigo Basins, a wind direction was along the long axis of the basin from the upper to the lower reaches of a river. Concerning wind speed, it was more than 1.0 m/s along the Tone and western part of Kanto Plain, and was more than, 1.5 m/s in the northern part of Chiba Prefecture. In the mountainous area on the west side of the Kanto Plain, the wind speed was less than 1.0 m/s, and was less than 0.5 m/s in the Chichibu, Nakanojo, Numata and Daigo Basins.

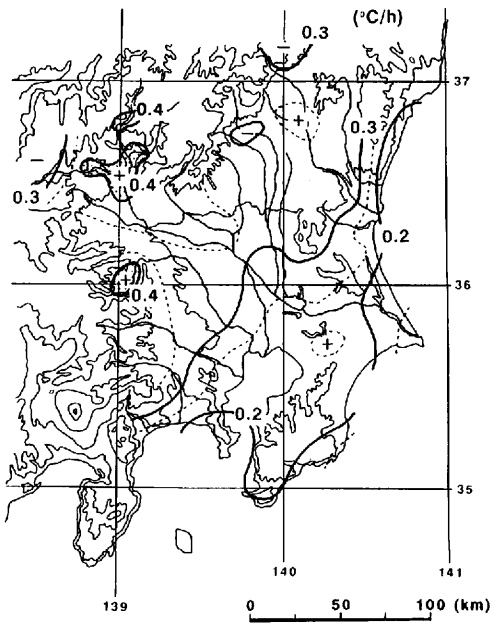

Fig. 5.2 The spatial distribution of the monthly averaged cooling rate (℃/h) for May, 1986.

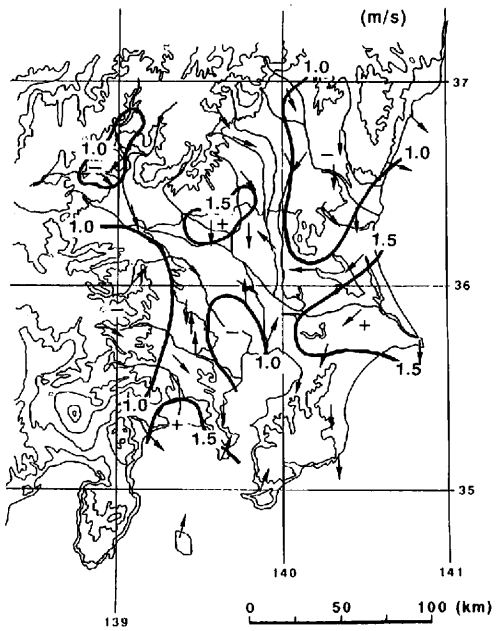

Fig. 5.3 The spatial distribution of wind direction of the highest frequency and the monthly averaged wind speed (m/s) for May, 1986.

As mentioned in Chapter 3.1, cooling rate had a close relation to net radiation all through the night indicating the strength of radiative cooling at ground surface, and it was expected that there existed also a close relationship between the spatial distribution of cooling rate and that of net radiation. But there are no available data about net radiation. So an attempt as follows was made to estimate the amount of net radiation. The sum of duration hours of sunshine two hours before sunset (between 1700 and 1900) and two hours after sunrise (between 0500 and 0700) was defined as clear-night index. This index had large value

at a clear night when strong radiative cooling was considered to be occurred. Fig. 5.4 shows the relationships between clear-night index and net radiation of the nighttime observed at Tsukuba in May, 1986. The correlation coefficient was −0.91 (significant level 0.1 %), and it is known that this index expressed the amount of net radiation and the strength of radiative cooling at ground surface.

Fig. 5.5 shows the spatial distribution of the monthly averaged clear-night index in the Kanto District in May, 1986. This index was more than 1 hours in the northern part and west side of Kanto Plain. Conversely, this index was less than 0.8 hours in the southern part of Kanto Plain.

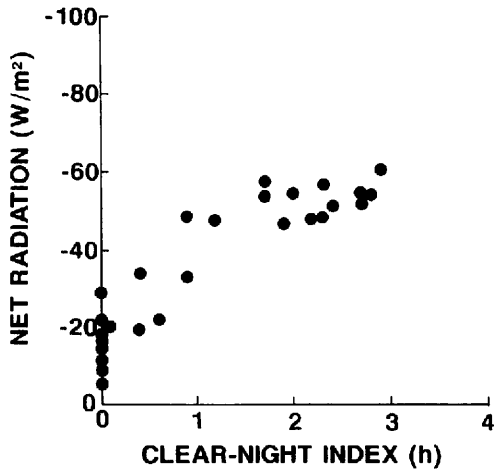

Fig. 5.4 The relationships between clear-night index and net radiation through the night at the Aerological Observatory for May, 1986.

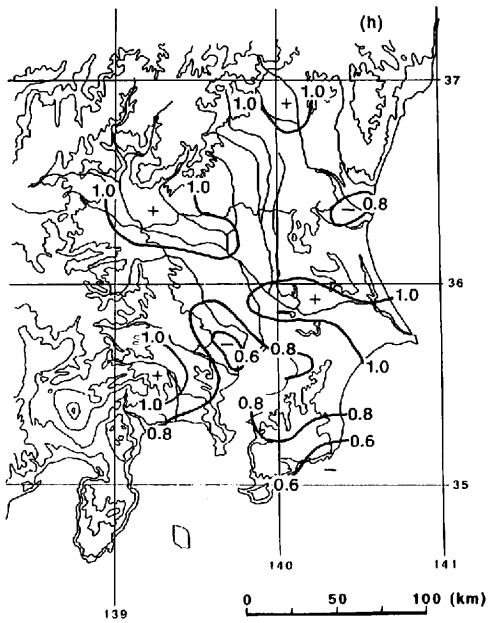

Fig. 5.5 Spatial distribution of clear-night index (h) for May, 1986.

Comparing the spatial distribution of the cooling rate with that of the clear-night index, they had large values in the northern part and west side of Kanto Plain. However, the clear-night index was large but cooling rate was small on the lower Tone river. In this area in May, 1986, the wind speed was more than 1.5 m/s. as shown in Fig. 5.3. So it was considered that this is the reason why cooling rate was small against to the large value of the clear-night index in this area.

Fig. 5.6 shows the relationships between the clear-night index and the monthly mean of cooling rate in Kanto District in May, 1986. To consider wind speed of each sites, the only observation station, where the height of the anemometer was 6.5 m high above the earth's surface, were used and plotted in this figure. The cooling rate tended to increase with clear-night index being large in the sites where wind was weak (less than 1.0 m/s) and tended to be small in windy sites, and these conditions were similar to that shown in Chapter 3.1.

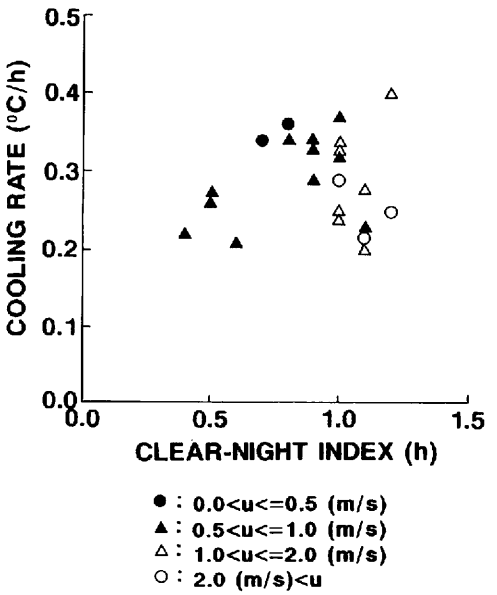

Fig. 5.6 The relationships between clear-night index and cooling rate for May, 1986.

5.2 The relationships between topographical features and nocturnal cooling in basins in the Tohoku and Chubu Districts

The time variation of air temperature all through the night depended on the radiative cooling and advection of cold air from the surrounding slope in the Sugadaira Basin as mentioned in Chapter IV. This cooling is considered to occur in any other basins. But these basins have their own topographical features, so the time variation of the air temperature observed in the basin was influenced by them. The relationships between the topographical shape of basin and the variation of air temperature during the night in the basin. At first, the topographical shape of the basin was illustrated as follows. Fig. 5.7 shows a simple model indicating the shape of a basin. Here S_b was the size of the bottom of the basin, S_r the size of the area surrounded by the ridge of the basin, h the mean relative height of the ridge, L_{bl} and L_{bs} the length of the long axis and the short axis of the bottom of the basin, L_{rl} and L_{rs} the length of the long axis and the short axis of the area surrounded by the ridge of the basin, respectively. The shape of the basin was expressed

by these seven parameters. Fig. 5.8 shows the locations of the basin in the Tohoku and Chubu Districts analyzed and Table 5.1 shows the parameters of the analyzed basins. These parameters were estimated by the use of topographical maps with a scale of 1:50,000 and 1:200,000.

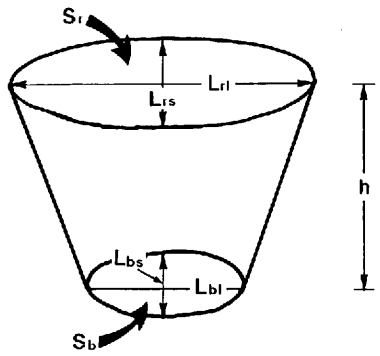

Fig. 5.7 A simple model indicating the shape of the basin.

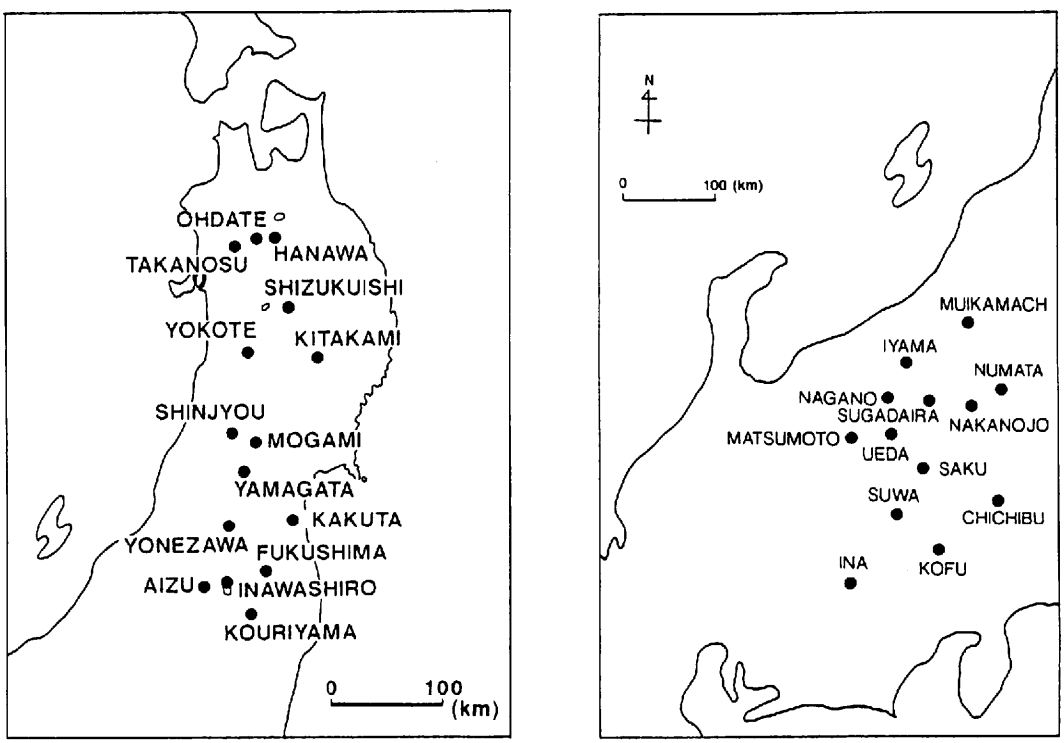

Fig. 5.8 The locations of the basins analysed in Tohoku and Chubu Districts.

Table 5.1 The parameters of the shape of the basins (Tohoku District).

	name of basin	h (m)	L_{bl} (km)	L_{bs} (km)	L_{rl} (km)	L_{rs} (km)	S_b (km^2)	S_r (km^2)
1	Takanosu	570	28.9	14.6	77.1	28.6	119.9	1574.1
2	Odate	430	20.6	14.9	50.9	24.0	135.1	674.9
3	Hanawa	570	30.3	9.4	54.9	31.4	66.4	920.1
4–6	Yokote							
4	Omagari	800	73.4	33.7	125.1	49.7	863.4	3797.3
5	Yokote	770	73.4	33.7	125.1	49.7	863.4	3797.3
6	Yuzawa	730	73.4	33.7	125.1	49.7	863.4	3797.3
7	Shinjyo	480	26.9	22.9	52.3	34.6	313.8	1154.9
8	Mogami	640	13.1	8.6	26.3	20.9	50.7	325.8
9–12	Yamagata							
9	Obanasawa	630	19.4	15.4	36.9	27.1	133.0	546.4
10	Tateoka	870	45.1	28.0	56.6	54.3	476.2	1858.7
11	Aterasawa	830	45.1	28.0	56.6	54.3	476.2	1858.7
12	Yamagata	820	45.1	28.0	56.6	54.3	476.2	1858.7
13–15	Yonezawa							
13	Nagai	590	21.7	10.6	30.0	23.7	120.6	416.5
14	Takabatake	660	28.9	21.7	55..4	31.7	290.8	998.2
15	Yonezawa	640	28.9	21.7	55.4	31.7	290.8	998.2
16–17	Aizu							
16	Kitakata	790	39.1	13.7	62.9	25.1	300.8	950.6
17	Wakamatsu	790	39.1	13.7	62.9	25.1	300.8	950.6
18	Shizukuishi	730	18.9	10.9	41.1	23.4	106.6	667.3
19–24	Kitakami							
19	Morioka	520	30.3	13.1	39.4	30.3	242.0	739.2
20	Shiba	510	30.3	13.1	39.4	30.3	242.0	739.2
21	Kitakami	680	54.0	24.9	70.0	61.1	645.2	2514.4
22	Wakayanagi	640	54.0	24.9	70.0	61.1	645.2	2514.4
23	Esashi	700	54.0	24.9	70.0	61.1	645.2	2514.4
24	Ichinoseki	370	14.0	11.1	40.0	26.8	59.2	603.0
25	Kakuta	280	17.7	9.1	29.1	16.0	86.5	351.7
26–27	Fukushima							
26	Yanagawa	730	32.3	16.3	50.6	41.1	251.5	1144.0
27	Fukushima	710	32.3	16.3	50.6	41.1	251.5	1144.0
28	Inawashiro	520	28.4	15.4	40.3	26.0	226.3	624.3
29	Kouriyama	460	54.0	24.0	54.9	51.1	531.2	1772.9

Table 5.1 (continued)
(Chubu and Kanto District)

	name of basin	h (m)	L_{bl} (km)	L_{bs} (km)	L_{rl} (km)	L_{rs} (km)	S_b (km^2)	S_r (km^2)
30–31	Muikamachi							
30	Koide	860	44.6	12.6	55.6	24.0	191.7	895.7
31	Yuzawa	610	44.6	12.6	55.6	24.0	191.7	895.7
32	Iiyama	750	23.4	9.8	31.4	21.0	93.3	1250.0
33	Nagano	830	44.8	13.6	52.2	35.2	297.6	1044.9
34–35	Matsumoto							
34	Omachi	890	55.2	17.8	71.2	34.6	441.7	1250.4
35	Hodaka	1140	55.2	17.8	71.2	34.6	441.7	1250.4
36–37	Ueda							
36	Ueda	590	18.0	14.8	28.4	22.2	90.9	353.3
37	Tobumachi	870	18.0	14.8	28.4	22.2	90.9	353.3
38	Saku	520	17.6	12.4	35.4	24.4	102.8	488.2
39	Suwa	920	14.8	4.0	35.0	25.0	57.5	530.3
40–42	Ina							
40	Tatsuno	680	64.8	19.0	79.0	24.4	317.7	1336.2
41	Ijima	670	64.8	19.0	79.0	24.4	317.7	1336.2
42	Ida	920	64.8	19.0	79.0	24.4	317.7	1336.2
43–46	Kofu							
43	Nirasaki	1150	31.8	31.4	56.2	49.2	352.8	1450.4
44	Kofu	1230	31.8	31.4	56.2	49.2	352.8	1450.4
45	Katsunuma	1120	31.8	31.4	56.2	49.2	352.8	1450.2
46	Nakatomi	1280	31.8	31.4	56.2	49.2	352.8	1450.2
45*	Numata	590	18.6	14.2	35.6	25.6	80.3	418.1
46*	Nakanojo	570	14.4	9.0	27.8	22.0	48.8	266.9
47*	Chichibu	710	14.0	11.0	31.2	22.2	63.0	483.9
(48)	sugadaira	360	4.5	1.3	10.4	4.8	3.4	28.2

*:Kanto District

The angle of the surrounding slope α and the exposure to the sky at the center of the basins β were obtained as follows:

$$tan\ \alpha = \frac{h}{\frac{L_{rm} - L_{bm}}{2}}, \quad tan\ \beta = \frac{h}{\frac{L_{rm}}{2}}, \tag{5.2}$$

where,

$$L_{rm} = \frac{L_{rl} + L_{rs}}{2}, \quad L_{bm} = \frac{L_{bl} + L_{bs}}{2}. \tag{5.3}$$

α, β obtained the above equations were shown in Table 5.2.

Table 5.2 The slope angle α and the exposure to the sky $\hat{\beta}$ of the surrounding slope (Tohoku District).

	name of basin	α (°)	$\hat{\beta}$ (°)
1	Takanosu	2.1	0.62
2	odate	2.5	0.66
3	Hanawa	2.8	0.76
4–6	Yokote		
4	Omagari	2.7	0.53
5	Yokote	2.6	0.50
6	Yuzawa	2.5	0.48
7	Shinjyo	3.0	0.63
8	Mogami	5.7	1.55
9–12	Yamagata		
9	Obanasawa	4.9	1.13
10	Tateoka	5.3	0.90
11	Aterasawa	5.0	0.86
12	Yamagata	5.0	0.85
13–15	Yonezawa		
13	Nagai	6.3	1.25
14	Takabatake	4.1	0.87
15	Yonezawa	4.0	0.84
16–17	Aizu		
16	Kitakata	5.1	1.03
17	Wakamatsu	5.1	1.03
18	Shizukuishi	4.8	1.29
19–24	Kitakami		
19	Morioka	4.5	0.85
20	Shiba	4.5	0.85
21	Kitakami	3.0	0.60
22	Wakayanagi	2.8	0.56
23	Esashi	3.1	0.61
24	Ichinoseki	2.0	0.64
25	Kakuta	3.5	0.71
26–27	Fukushima		
26	Yanagawa	3.9	0.91
27	Fukushima	3.8	0.89
28	Inawashiro	5.3	0.90
29	Kouriyama	3.8	0.50

Table 5.2 (continued)
(Chubu and Kanto District).

	name of basin	α (°)	β (°)
30–31	Muikamachi		
30	Koide	3.0	0.60
31	Yuzawa	3.0	0.60
32	Iiyama	2.5	0.66
33	Nagano	2.8	0.76
34–35	Matsumoto		
34	Omachi	2.7	0.53
35	Hodaka	2.5	0.48
36–37	Ueda		
36	Ueda	2.6	0.50
37	Tobumachi	3.0	0.63
38	Saku	4.9	1.13
39	Suwa	5.3	0.90
40–42	Ina		
40	Tatsuno	5.0	0.86
41	Ijima	5.0	0.86
42	Ida	6.3	1.25
43–46	Kofu		
43	Nirasaki	4.1	0.87
44	Kofu	4.0	0.84
45	Katsunuma	5.1	1.03
46	Nakatomi	5.1	1.03
45*	Numata	4.5	0.85
46*	Nakanojo	4.5	0.84
47*	Chichibu	3.0	0.60
(48)	Sugadaira	8.7	5.42

*:Kanto District

Table 5.3 shows the correlation coefficients between topographical shapes of the basin and cooling rate at the bottom of the basins. In this table, the significant relationships were (1) between cooling rate and h (the correlation coefficient 0.32, and significant level 5 %), and (2) between cooling rate and $tan\ \alpha$ (0.40 and 1 %). The relationship (1) meant that cooling rate became larger with increasing relative height of the surrounding mountain. Since α indicated the inclination of the slope surrounding the basin, the relationship (2) meant that cooling rate became larger with increasing inclination of the slope.

It was stated in the previous chapters that time variation of air temperature in the basin during the night depended on the radiative cooling, and turbulence and advection of cold air from the surrounding slopes. Therefore, the relationships between the radiative cooling and the topographical shape of basins was considered at first. As the bottom of the basin is surrounded by the mountain slopes, the effect of the slope on the radiation balance at the bottom should be tested. According to the results of calculation from

Eqs. (5.2) and (5.3), the angles of the slopes and the exposure to the sky at the center of the basins were very small as shown in Table 5.2. The average angle of the mountain slopes is about 3.9 degree and the average of the exposure to the sky about 0.81 degree. Therefore, the proportion of the screening of the radiation is less than 1 % and the effects of the slope on the radiation balance at the bottom are negligible.

The relationships between cooling rate and height above sea level is shown in Fig. 5.9. Cooling rate tended to increase with increasing height above sea level. This is because the drop of air temperature and decrease of vapor amount in the air layer with increasing height led to the increase of net radiation lost by the earth's surface and the strengthening of radiative cooling. Here, two star-asterisks indicated the

Table 5.3 The correlations between geographical shapes and cooling rate in basins.

	h	L_{bl}	L_{bs}	L_{bm}
cooling rate	0.32*	-0.17	-0.18	-0.19

	L_{rl}	L_{rs}	L_{rm}
cooling rate	-0.31*	-0.14	-0.28

	S_h	S_r	$tan\ \alpha$	$tan\ \beta$
cooling rate	-0.24	-0.36**	0.41***	0.35**

*significant level *5 %
**2 %
***1 %

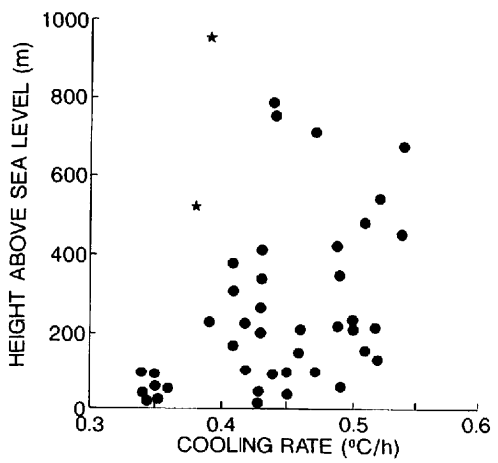

Fig. 5.9 The relationships between cooling rate and height above sea level at the bottom of the basin.
★: The station located near the lake.

values of Inawashiro and Suwa. This two places were located near the big lakes named Inawashiro-ko, and Suwa-ko, so cooling rate was small by the effect of big lakes. Kondo (1982) made clear the relationships between cooling rate and height above sea level by analysing the AMeDAS date in Fukushima, Miyagi, and Yamagata Prefectures. This facts supported the results shown in Fig. 5.9.

Secondly, it was considered about the relationships between the atmospheric cooling in the basin and the area of the surrounding slopes which forms the cold air flowing down into the basin and cooling its air layer. Now, supposing that the cold air formed on the slopes having an area S_s flows into the air layer with height h_a above the bottom of the basin having an area S_b, and cools this air layer by ∂T in time t, the following equation was made up.

$$t \cdot H \cdot S_s = C_p \cdot \rho \cdot \partial T \cdot S_b \cdot h_a, \tag{5.4}$$

where, t was equal to the duration time of the night, H the sensible heat flux on the slope, C_p the specific heat of air at constant pressure, ρ the density of air. Finally this equation became

$$\partial T = \frac{1}{C_p} \cdot \rho \cdot h_a \cdot t \cdot H \frac{S_s}{S_b} \cdot \tag{5.5}$$

In these terms, only S_s/S_b had the relation to the topographical shape of the basin. Fig. 5.10 shows the relationship between S_s/S_b and cooling rate at the bottom of the basin. Cooling rate became higher strikingly in accordance with increasing S_s/S_b, even through the points were scattered. This indicated that as S_s/S_b becomes large, that is, the amout of the advection of cold air formed on the slope was large, so the stmospheric cooling at the bottom of the basin became intensive.

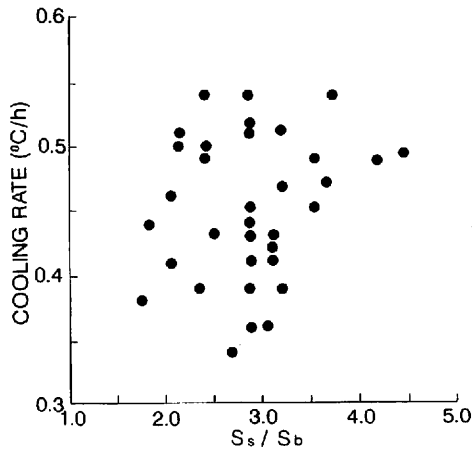

Fig. 5.10 The relationship between S_s/S_b and cooling rate at the bottom of the basin.

The relationship between the angle of the surrounding slopes and cooling rate at the bottom of the basin is shown in Table 5.3 and illustrated in Fig. 5.11. As mentioned above, the correlation coefficient was 0.42 (significant at the level 1 %). The relationship can be explained as follows: The cooling in the basin depended on to the advection of cold air, and this advected air was supplied by the cold air drainage flowing down on the slopes surrounded. The amount of the supply was related to the speed of cold air drainage (Kondo, 1982) and this speed was proportional to the angle of slope. So it is considered that as the angle of the slope became large, the wind speed of cold air drainage became higher and the amount of the supply of cold air became abundant. As a result, cooling rate became large in the basin.

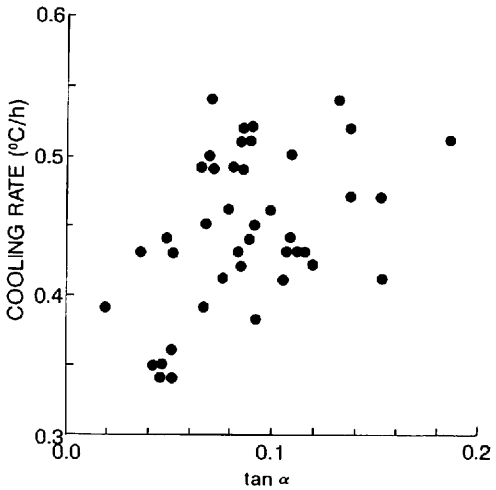

Fig. 5.11 The relationship between *tan* α and cooling rate at the bottom of the basin.

CHAPTER VI

DISCUSSION

In Chapters III to V, the characteristics of nocturnal decline of air temperature in plains and basins were mentioned, and in this chapter, they are intended to be compared and discussed. Table 6.1 shows cooling rate and wind speed when a surface inversion layer was formed. Tsukuba represented the place located on a plain and Sugadaira represented the location at the bottom of a basin, and these values, obtained by the intensive observations on the plain and in the basin, were mean values during the nights when they were carried out. Cooling rate was larger in the basin than on the plain, and the value of the former was 1.4 times as much as that of the latter. On the other hand, wind speed was larger on the plain than in the basin, and this same tendency was shown about the monthly mean values of cooling rate and wind speed.

Table 6.2 shows the monthly means of cooling rate and wind speed on the plain and in the basins in the Kanto District for May, 1986. Observation points in the basins were Daigo, Numata, Nakanojo and Chichibu Basins. The value of cooling rate of the basins was 1.7 times larger than that of the plain. Conversely, the value of wind speed of the plain was about 1.8 times larger than that of the basins. This is because the shape of the basins weakened the invasion of the general wind in the upper air layer, so in the basin, the heating due to the vertical convection was restrained and the cooling strengthened relatively. This effect was called the "blocking effect" of the surrounding mountains (Maki *et al.*, 1986).

Concerning the time variation of air temperature and the mechanics of the nocturnal cooling in the surface inversion layer on a clear night, the basin differed from the plain. Table 6.3 shows the one-night mean values of the time variation of air temperature in Tsukuba and Sugadaira. These values were obtained from the analyzed results in Chapters III and IV. The observed cooling, which is the same as cooling rate defined in this study, on the plain was about 2/3 of the value of the basin. Referring about the mechanics of the nocturnal cooling in the surface inversion layer on the plain in more detail, the ratio of radiative cooling

Table 6.1 Nocturnal mean values of cooling rate and wind speed in the surface inversion layers on a plain (Tsukuba) and in a basin (Sugadaira) (May 7–10, 1982).

	Tsukuba	Sugadaira
cooling rate (°C/h)	0.41	0.58
wind speed (m/s)	2.7	0.8

Table 6.2 Monthly mean values of cooling rate and nocturnal wind speed near the earth's surface on plains and in basins in the Kanto District (May, 1986).

	plain area	basin area
cooling rate (°C/h)	0.27	0.44
wind speed (m/s)	1.6	0.9

Table 6.3 Nocturnal mean values of heat balance components indicated by the variation of air temperature in surface inversion layers on the plain (Tsukuba) and in the basin (Sugadaira) (May 7–10, 1982).

	Tsukuba	Sugadaira
actual cooling (℃/h)	0.41	0.58
radiative cooling (℃/h)	0.32 (0.8)*	0.40 (0.7)*
turbulent and advective cooling (℃/h)	0.09 (0.2)*	0.18 (0.3)*

*Ratio to actual cooling.

to the observed cooling was about 80 %. The surface inversion layer was heated due to the vertical convection between this layer and upper air layer, and this heating weakened the effect of the turbulent cooling. So the ratio of radiative cooling to the observed cooling becomes relatively large.

There are several reports about the time variation of air temperature in the surface inversion layer on another plains. Andre and Mahrt (1982) showed that turbulent cooling and radiative cooling contributed comparably to cooling in this layer. Stull (1983) reported that about 77 % of observed cooling of the nocturnal boundary layer could be accounted for by the turbulent cooling and 23 % by atmospheric rediative cooling. Li *et al.* (1983) showed that cooling due to turbulent heat flux divergence could be ignored as compared with atmospheric radiative cooling.

On the other hand, the proportion of radiative cooling to total observed cooling in the basin was 70 %, and the effect of turbulent and advective cooling was stronger than on the plain. This is because, in the basin, there were the surrounding slopes which formed cold air, and because cold air drainage flowing down on the slope transferred this cold air to the air layer above the bottom of the basin.

Concerning about the time variation of air temperature in the surface inversion layer formed in another basins, Mori *et al.* (1983) showed that about 50 % of the total cooling in this layer was due to advection and accumulation of the cold air layer from surrounding mountain slopes from the analysis of the variation of air temperature in the air layer from the surface to 500 m high in Kawatabi, Miyagi Prefecture. Maki *et al.* (1986) reported from the observation at Akaigawa Basin in Hokkaido that about 80 % of the total cooling was advection of the cold air from surrounding slopes. The proportion of the advective cooling to the total cooling, that is, observed cooling in the Sugadaira Basin was estimated to be about 30 % and smaller than those mentioned above. This is considered to be because the meso-scale wind temporarily strengthened and heated the inversion layer at midnight, and so the effect of the advective cooling all through the night was small.

Finally, the mechanics of the nocturnal cooling on the slope which played an important role in the atmospheric cooling in the basin was discussed. Table 6.4 shows the amount of observed cooling and radiative cooling in the air layer near the earth's surface on the slope at a clear night when the surface inversion layer was formed in the basin. The actual cooling was about 0.42 ℃/h, but the radiative cooling was estimated to be about 1.34 ℃/h, and it is larger than the actual cooling. This suggested that the air layer on the slope was heated due to the turbulence and advection of warm air. On the slope, the air cooled due to atmospheric radiative cooling flew along the slope to the bottom of the basin. After it flew out, the warm air flew from upper air layer and replaced, that is, the warm air advected from upper air layer compensated for the cold air flowing off along the slope. Moreover, this replaced air was cooled and flew off with its gravity. This condition was described as a part of the circulation formed in basins at a clear and calm night (Mano, 1953, 1956; Vorontsov, 1958; Kimura, 1961; Kudo *et al.*, 1982).

Because of the mechanism as mentioned above, wind speed and air temperature on a slope changed periodically. Toritani (1985) reported by spectrum analysis that this period is 60–90 minutes. It indicated that outflow of cold air and inflow of warm air near the earth's surface on the slope occurred periodically and its periodicity is 60–90 minutes, and as a result, cooling rate on the slope was lower than that of the bottom of the basin.

Table 6.4 Nocturnal mean values of heat balance components indicated by the variation of air temperature in the surface inversion layers on and above the slope at Sugadaira (May, 7–10, 1982).

actual cooling (℃/h)	0.42
radiative cooling (℃/h)	1.34

CHAPTER VII

CONCLUSIONS

At clear nights, the air near the ground surface was cooled. Defining the strength of this atmospheric cooling as cooling rate, it depended mainly on the strength of radiative cooling at the surface indicated by net radiation, and there was a good correlation between them when wind speed is less than 1.0 m/s. When cooling rate became high, the air temperature gradient became positive and high values, and this indicated that the inversion layer of air temperature was formed in the air layer near the surface.

On a plain, the thickness of this inversion layer reaches about 100 m high above ground level. At Tsukuba, three sub-layers were distinguished in the air layer from the surface to 200 m. The lowest sub-layer was a strong inversion layer (from the surface to 25 m). The middle sub-layer was a weak inversion layer (from 25 to 100 m). The upper sub-layer was about neutral stratification and the meso-scale wind prevails in it (from 100 to 200 m). By computing the heat balance in these air layers, it was made clear that the time variation of air temperature depended mainly upon radiative cooling, and turbulent and advective heating in the lowest sub-layer, but mainly upon radiative cooling, and turbulent and advective cooling in the middle and upper sub-layers.

In a basin, wind speed was lower than on a plain by the "blocking effect", and a strong surface inversion layer called cold air lake was formed. At Sugadaira, the thickness of the surface inversion layer reached 70–80 m high. Three sub-layers were distinguished in the same manner as at Tsukuba. The lowest sub-layer was a strongly stable layer and the air temperature fell down all through the night (from surface to 40 m). The middle sub-layer was a weak stable layer and the air temperature rose temporarily at midnight (from 40 to 80 m). The upper sub-layer was almost neutral stratification and the meso-scale wind prevailed in this layer (from 80 to 200 m). By computing the heat balance in these air layers, it was clear that about 60–70 % of atmospheric cooling was radiative cooling, and the other part of the variation of air temperature was considered to be due to turbulent and advective cooling in the lowest and middle sub-layers. By the isentropic analysis in the air in the basin, and by the observation results about the vertical distribution of wind direction and speed, this turbulent and advective cooling in these air layer was considered to be caused by the air flow from the surrounding slope.

Concerning some topographical characteristics of the cooling rate in the plain, it was high where the radiative cooling at the earth's surface is strong, when wind speed is less than 1.0 m/s. On the other hand, the cooling rate tended to become higher in a basin with high altitude, large inclination of the surrounding slopes, and broad area size of these slope as compared with that of the bottom of the basin. On these slope, cold air dropping down air temperature in the basin was formed.

Finally, concerning the difference of the time variation of the air temperature in the surface inversion layer formed during the night, between on a plain and in a basin, the observed cooling in the basin was estimated to be about 1.4 times higher than on the plain. In detail, radiative cooling in the basin was about 1.3 times higher than on the plain, and turbulent and advective cooling in it was about twice higher. This is because the basin was located in the place with high altitude and had the surrounding slopes which formed cold air, and because cold air drainage which flew down on the slope and transferred this cold air to the air layer above the bottom of the basin.

ACKNOWLEDGEMENTS

The author wishes to express his gratitude to his academic adviser, Dr. Masatoshi Yoshino, Professor in the Institute of Geoscience, University of Tsukuba, for a lot of helpful guidance, suggestions and encouragements throughout the study. He wishes also to acknowledge the advice of Profs. T. Kawamura, T. Nishizawa, and K. Kotoda of the Institute of Geoscience, University of Tsukuba. He is grateful to Drs. M. Kobayashi, T. Yasunari, S. Yamakawa, H. Ikeda, J. Shimada and F. Iseya of the Institute of Geoscience, University of Tsukuba, and Dr. Y. Hayashi of National Institute of Agro-Environmental Science in Tsukuba. Thanks are also due to Dr. K. Shibata of the Meteorological Research Institute, Dr. T. Ueno and Mr. M. Ito of the Aerological Observatory, Japan Meteorological Agency in Tsukuba.

His heartfelt thanks are due to Mr. M. Nasuno, Misses T. Murakami, M. Awakura, and A. Yatagai for typing this paper and drawing these figures and tables.

In preparing this presentation, the author had many supports with his colleagues, Dr. M. Taniguchi, Mr. R. Kawamura and H. Iijima of the Environmental Research Center. Thanks are also to Dr. R. Wittrup for English wording of the manuscript.

REFERENCES

Aida, M. (1982): *Taiki to houshakatei*. Tokyo-do, Tokyo, 281p (in Japanese).

Aichele, H. (1953): Kaltluftpulsationen. *Met. Rdsch.*,**8**, 53-54.

Andre, J. C. and Marhrt L. (1982): The nocturnal surface inversion and inflluence of clear-air radiative cooling. *Jour. Atmos. Sci.*, **39**, 864-878.

Atkinson, B. W. (1981): *Meso-scale atmospheric circulation*. Academic Press, London, 495p.

Baumgartner, A. (1962): Die Lufttemperatur als Standorts-faktor am Gr. Flakenstein. *Mitt. Forstw. Cbl.*, **81**, 17-47.

Bergen, J. D. (1969): Cold air drainage on a forested mountain slope. *Jour. Appl. Met.*, **8**, 884-895.

Buettner, K. J. K. and Thyer, N. (1966): Valley winds in the Mount Rainier area. *Arch. Met. Geoph. Biokl., Ser. B*, **14**, 125-147.

Doran, J. C. and Horst, T. W. (1981): Velocity and temperature oscillations in drainage winds. *Jour. Appl. Met.*, **20**, 361-364.

Elsasser, W. M. (1942): *Heat transfer by infrared radiation in the atmosphere*. Harvard Met. Studies. No.6, 107p.

Fleagle, R. G. (1950): A theory of air drainage. *Jour. Met.*, **7**, 227-232.

Geiger, R. (1965): *The climate near the ground*. Harvard Univ. Press, Cambridge, Mass., 611p.

Garratt, J. R. and Brost, R. A. (1981): Radiative cooling effects within and above the nocturnal boundary layer. *Jour. Atmos. Sci.*, **38**, 2730-2746.

Hanna, S. R. (1969): The thickness of the planetary boundary layer. *Atmos. Environ.*, **3**, 519-536.

Harimaya, T., Maki, M., Kikuchi, K., Taniguchi, T., Ohira, T. and Yoshihiro, M. (1985): Observation of nocturnal cooling in Akaigawa basin, Hokkaido. *Geoph. Bull. of Hokkaido Univ.*, No.45, 29-41 (in Japanese with English abstruct).

Ishibashi, T. and Numata, Y. (1965): On the captive balloon observation at Tateno (1st report). *Jour. Met. Res.*,**17**, 595-602 (in Japanese with English abstruct).

Katayama, A. (1972): A simplified scheme for computing the radiative transfer in the troposphere. Numerical simulation of weather and climate. *Technical Report*, **No.6**, Dept. Met. UCLA, 77p.

Kimura, H. (1961): A micrometeorological study on small islands. Micrometeorological surveys at Hakatajima and Oshima-small islands in the Inland Sea of Seto. Met. Note, *Met. Res. Ins., Kyoto Univ., Ser. 2*, **No.22**, 1-60, 1-140.

Kobayashi, S. and Ishikawa, N. (1982): Cold air flow on the snow surface. *Low Temp. Sci., Ser. A*, **No.41**, 55-64 (in Japanese).

Kondo, J. (1982): Preliminary theoretical study on nocturnal cooling over complex terrain. *Tenki*, **29**, 935-949 (in Japanese).

Kondo, J. (1984): Effect of the topographical and ground surface conditions on the nocturnal drainage wind and cooling in mountainous region (Part 1). *Tenki*, **31**, 625-632 (in Japanese).

Kondo, J. and Kuwagata, T. (1984): A relation between the depth of nocturnal stable layer (cold-air-pool) and the topographical depth of the basin. *Tenki*, **31**, 1094-1102 (in Japanese).

Kudo, T., Tanaka, H., Toritani, H. and Hwang, S. (1982): Formation of cold air lake in Sugadaira Basin. *Geog. Rev. Japan*, **55**, 849-856 (in Japanese with English abstruct).

Li, X., Gaynor, J. E. and Kaimal, J. C. (1983): A study of multiple stable layers in the nocturnal lower atmosphere. *Bound.-Layer Met.*, **26**, 157-168.

Magono, C. and Nakamura, C. (1982): Nocturnal cooling of the Moshiri basin, Hokkaido in midwinter. *Jour. Met. Soc. Japan*, **60**, 1106-1116.

Mahrt, L., Heald, L. R. C., Lenschow, D. H., Stankov, B. B. and Troen, I. B. (1979): An observational study of the

structure of the nocturnal boundary layer. *Bound.-Layer Met.*, **17**, 247-264.

Maki, M., Harimaya, T., Kikuchi, K., Taniguchi, T. and Horie, N. (1984): Process of nocturnal cooling in a land basin. *Geoph. Bulla. Hokkaido Univ.*, **43**, 17-29 (in Japanese with English abstruct).

Maki, M., Harimaya, T. and Kikuchi, K., (1985 a): Nocturnal cooling systems in basin. (1) Heat balance analysis. In: The study of mechanism and quantitative prediction of occurrence of the extraordinary cooling in boundary layer as a primary factor of the damage of crops. ed. by Kondo, J., *Report of Research Group of Natural Disasters*, No. A-60-4, 192-215 (in Japanese).

Maki, M., Harimaya, T. and Kikuchi, K., (1985 b): Nocturnal cooling systems in basin. (2) Effects of cold air drainage. In: The study of mechnism and quantitative prediction of occurrence of the extraordinary cooling in boundary layer as a primary factor of the damage of crops. ed. by Kondo, J., *Report of Research Group of Natural Disasters*, No. A-60-4, 216-232 (in Japanese).

Maki, M., Harimaya, T. and Kikuchi, K., (1986): Heat budget studies on nocturnal cooling in a basin. *Jour. Met. Soc. Japan*, **64**, 727-741.

Mano, H. (1953): Sudden increase of nocturnal temperature in the valley and the basin. *Jour. Met. Res.*, **5**, 525-545 (in Japanese with English abstruct).

Mano, H. (1956): A study on the sudden nocturnal temperature rise in the valley and the basin. *Geoph. Mag.*, **27**, 169-204 (in Japanese).

Miura, K. (1971): An example of the formation of cold air lake. *Ann. Tohoku Geog. Ass.*, **23**, 37-40 (in Japanese).

Mihara Y., Tsuruta, K. and Nemoto, O. (1977): Frost Damage increased by the windbreak. *Jour. Agr. Met.*, **33**, 67-74 (in Japanese with English abstruct).

Mori, Y., Kondo, J., Shoji, K., Sato, T., Yasuda, N., Haginoya, N., Miura, A., Yamazawa. H., Kawanaka, A., Takahira, S. and Abe, E. (1983): Nocturnal cooling and heat balance at the mountain district. *Tenki*, **30**, 259-267 (in Japanese).

Nakamura, K. (1976): The nocturnal cold air drainage and distribution of air temperature on the gentle slope. *Geogr. Rev. Japan*, **49**, 380-387 (in Japanese with English abstruct).

Nakamura. K. (1983): Local Climatological Study of the nocturnal cold air drainage on the mountain slope. Dr. Sc. Thesis. Univ. of Tsukuba, Japan, 142p.

Nakamura, K. (1985): Vertical structure of nocturnal cold air drainage on the slopes of valley and basin. *Geogr. Rev. Japan*, **58**, 477-491 (in Japanese with English abstructw).

Nieuwstadt, F. T. M. and Tennekes, H. (1981): A rete question for the nocturnal boundary layer height. *Jour. Atmos. Sci.*, **38**, 1418-1428.

Nishiyama, H. (1985): Minimum temperature and radiation balance at Tateno. *Jour. Aero. Obser. Tateno*, No.45, 6-10 (in Japanese with English abstruct).

Nomoto, S (1982): Local anticyclines and cyclones in Japan. Dr. Sc. Thesis, Univ. of Tsukuba, Japan, 209p.

Ohata, T. and Higuchi, K. (1979): Gravity wind on a snow patch. *Jour. Met. Soc. Japan*, **57**, 254-263.

Oke, T. R. (1978): *Boundary Layer Climates*. Methuen & Co. LID. London, 372p.

Ota, I. (1960): Inversion and diffusion of fumes. *Kisho-Kenkyu Note*, **No.11**, 303-321 (in Japanese).

Perkovšek, Z. and Hočevar, A. (1971): Night drainage winds. *Arch. Met. Geoph. Biokl., Ser. A*, **20**, 353-360.

Sahashi, K. (1974): A simple theoretical treatment of the down slope wind. *Bull. School of Education, Okayama Univ.*, **40**, 17-25.

Schroeder, M. J. and Buck, C. C. (1970): *Fire weather*. U. S. Dep. Agr. Handbook. 360, Washington D. C., 229p.

Stull, R. B. (1983): A heat-flux history length scale for the nocturnal boundary layer. *Tellus*, **53A**, 219-230.

Suzuki, Y. (1977): Surface inversion at Tateno. *Jour. Met. Res.*, **29**, 113-116 (in Japanese with English abstruct).

Suzuki, Y., Akita, I. and Suzuki, T. (1978): Surface inversion at Tateno (II). *Jour. Aero. Obser. Tateno.*, **No.39**, 8-13 (in Japanese with English abstruct).

Tanaka, M. (1984): Formation of the stable layer and the local winds over the basin. *Dis. Pre. Res. Ins. Annc., Kyoto Univ.*, **No.27**, **B-2**, 107-119 (in Japanese with English abstruct).

Tanaka, M. and Edagawa, S. (1985): Cooling and formation of mountainwind in valley topograpry, in Chikuma river and Saku basin. In: The study of machnism and quantitative prediction of occurrence of the extraordinary cooling in boundary layer as a primary factor of the damage of crops. ed. by Kondo, J., *Report of Research Group of Natural Disasters*, No. A-60-4, 154-166 (in Japanese).

Tanaka, Y., Ishigaki, K., Fujiwara, K. and Kobayashi, D. (1982): Nocturnal cooling in the shallow valley and on the plateau. (1) Cooling process in the valley and on the side slope. *Jour. Agr. Met.*, **38**, 245-251 (in Japanese with English abstruct).

Thornthwaite, C. W. and Holtzman, B. (1939): The determination of evaporation from land and water surface. *Mon. Weath. Rev.*, **67**, 4-11.

Taniguchi, T., Kikuchi, K. Harimaya, T. and Maki, M. (1983a): Observations of planetary boundary layer by means of sonic rider in the cold season, Hokkaido Island, Japan. *Geoph. Bull. Hokkaido Univ.*, **No.42**, 27-35 (in Japanese with English abstruct).

Tohsha, M. (1953): Temperature inversion in the lower atmosphere. *Jour. Met. Res.*, **5**, 649-654 (in Japanese with English abstruct).

Toritani, H. (1985 a): Formation and cold air lake and cold air drainage in the Sugadaira Basin, Nagano Prefecture, Japan. *Geog. Rev. Japan*, Ser. A, **58**, 67-79 (in Japanese with English abstruct).

Toritani, H. (1985 b): The time changes in wind and temperature during the cold air drainage on a mountain slope. *Tenki*, **32**, 311-319 (in Japanese).

Tyson, P. D. (1968): Velocity fluctuation in the mountain wind. *Jour. Atom. Sci.*, **25**, 381-384.

Vorontsov, P. A. (1958 a): Aerologicheskie issledovaniia progranichnogo sloia atmosferi nad melkosopochnim repiefom zelinnik. *Trudy GGO*, **No.73**, 61-86.

Vorontsov, P. A. (1958 b): Nekotorie voprosi aerologicheskikh issledovaniia pogranichnogo sloia atmosferi (some questions on aerological observations of the atmospheric boundary layer), In: *Sovremenie Problemy Meteorologii Prizemnogo Sloia Vozdukha, Sbornik Statei*, 157-179, Leningrad, Glav. Geofiz Observatory.

Vorontsov, P. A. (1961): Metody aerologicheskikh issledovanii progranichnogo sloya atmonsfery. *Gidrometeoizdat, Leningrad*, 1-451.

Vorontsov, P. A. (1969): Micro aerologic studies of the lowest 300-m layer, *In: Microclimate of the USSR*. ed. by Gol'tsberg, I. A., IPST Press, Jerusalem, Israel, 158-236.

Wyngaard, J. C. (1975): Modeling the planetary boundary layer extension to the stable case. *Bound.-Layer Met.*, **9**, 441-460.

Yamada, T. (1979): Prediction of the nocturnal surface inversion height. *Jour. Appl. Met.*, **18**, 526-531.

Yoshino, M. M. (1961): *Shokiko*. Chijin-shokan, Tokyo, 274p (in Japanese).

Yoshino, M. M. (1975): *Climate in a small area*. Univ. Tokyo Press, Tokyo, 549p.

Yoshino, M. M. (1980): Research on damage due to cold air drainage from the view point of local climatology. *Saigai no Kenkyu*, **11**, 124-135 (in Japanese).

Yoshino, M. M. (1982): On the model of cold air lake and cold air drainage. In: Topographical and climatological studies on cold air drainage. ed. by Yoshino, M. M., Owada, M., Nakamura, K., Hayashi, Y., Tanaka, M. and Toritani, H., *Climatalogical and Meteorological Reports, Univ. of Tsukuba*, **No.6**, 37-39 (in Japanese).

Yoshino, M.(1986): *Shinpan Shokiko*. Chijin-shokan, Tokyo, 298p (in Japanese).

Yoshino, M. M., Tanaka, M. and Nakamura, K. (1981): Formation of a cold air lake and its effects on agriculture. *Jour. Natural Disaster Ser.*, **3**, 1-14.

Yoshino, M. M.,Hayashi, Y. and Toritani, H. (1982): The characteristics of the cold air drainage in Sugadaira. In: Topographical and climatological studies on cold air drainage. ed. by Yoshino, M. M., Owada, M., Nakamura,

K., Hayashi, Y., Tanaka, M. and Toritani, H., *Climatalogical and Meteorological Reports, UnivM. of Tsukuba,* **No.6**, 15-21 (in Japanese).

Young, F. D. (1921): Nocturnal temperature inversion in Oregon and California. *Mon. Wea. Rev.*, **49**, 138-148.

Yu, T-W. (1978): Determining height of the nocturnal boundary layer. *Jour. Appl. Met.*, **17**, 28-33.

Zeman, O. (1979): Parameterization of the dynamics of stable boundary layers and nocturnal jets. *Jour. Atom. Sci.*, **36**, 792-804.

Environmental Research Center Papers

No.1 (1982) Kenji KAI: Statistical characteristics of turbulence and the budget of turbulent energy in the surface boundary layer. 54p.

No.2 (1983) Hiroshi IKEDA: Experiments on bedload transport, bed forms, and sedimentary structures using fine gravel in the 4-meter-wide flume. 78p.

No.3 (1983) Yousay HAYASHI: Aerodynamical properties of an air layer affected by vegetation. 54p.

No.4 (1984) Shinji NAKAGAWA: Study on evapotranspiration from pasture. 87p.

No.5 (1984) Fujiko ISEYA: An experimental study of dune development and its effect on sediment suspension. 56p.

No.6 (1985) Akihiko KONDOH: Study on the groundwater flow system by environmental tritium in Ichihara region, Chiba Prefecture. 59p.

No.7 (1985) Chong Bum LEE: Modeling and climatological aspects of convective boundary layer. 63p.

No.8 (1986) Kazuo KOTODA: Estimation of river basin evapotranspiration. 66p.

No.9 (1986) Abdul Khabir ALIM: Experimental studies on transient behavior of capillary zone. 76p.

No.10 (1987) Michiaki SUGITA: Evaporation from a pine forest. 61p.

No.11 (1987) Hye-Sock PARK: Variations in the urban heat island intensity affected by geographical environments. 79p.

No.12 (1988) Hiroshi IKEDA and Fujiko ISEYA: Experimental study of hetergeneous sediment transport. 50p.

No.13 (1989) Hitoshi TORITANI: A local climatological study on the mechanics of nocturnal cooling in plains and basins. 62p.

発行　　平成2年3月25日

編集・発行者　筑波大学水理実験センター

〒305 つくば市天王台1－1－1

TEL 0298(53)2532 FAX (53)2530

印刷　ニッセイエブロ株式会社

東京都港区西新橋2－5－10